

AD-A036 214

WRIGHT STATE UNIV DAYTON OHIO

F/G 14/2

IN-SITU MEASUREMENTS OF GAS SPECIES CONCENTRATIONS IN SIMULATED--ETC(U)

NOV 76 C CHANG, G D SIDES, T O TIERNAN

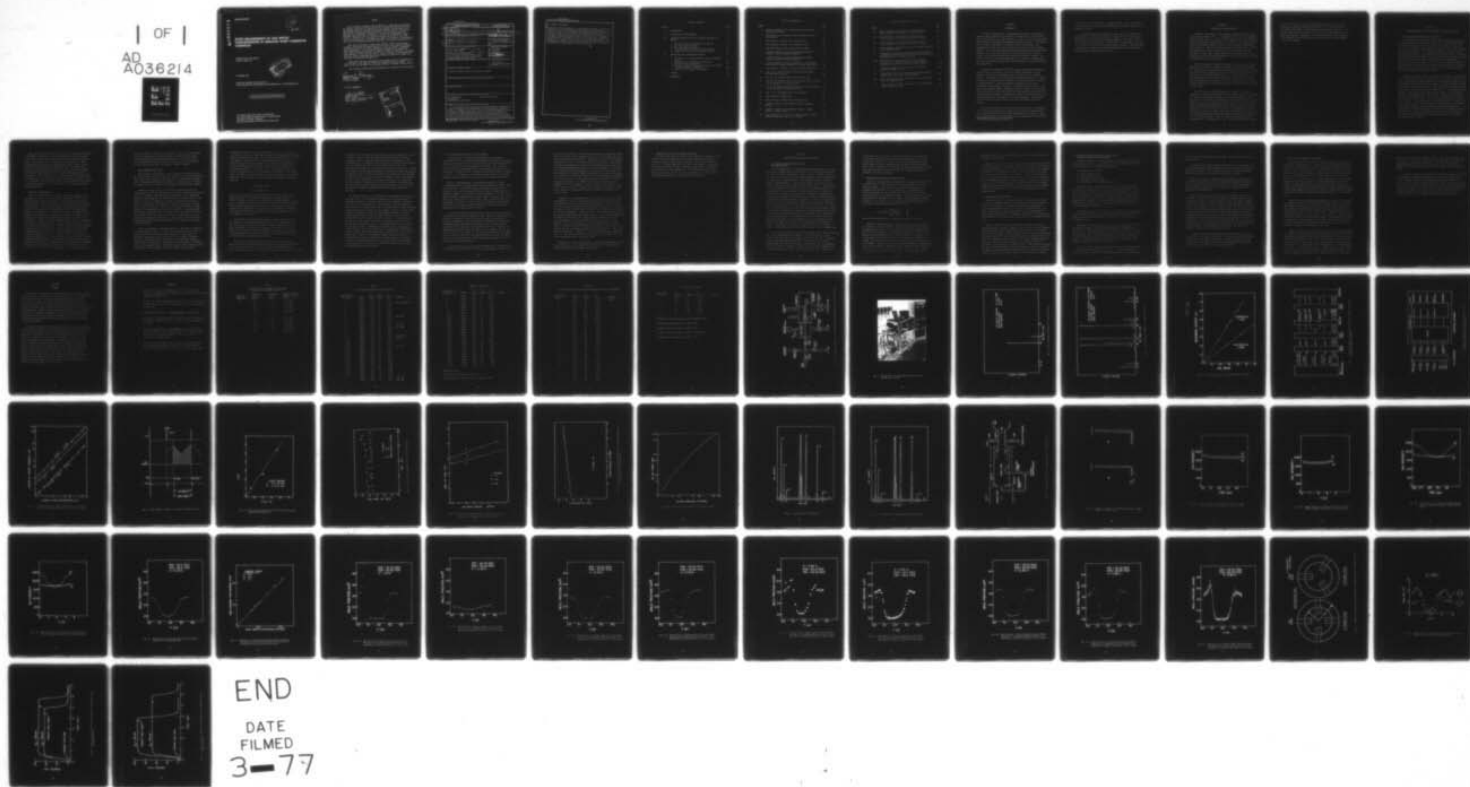
F33615-76-C-2010

UNCLASSIFIED

AFAPL-TR-76-105

NL

1 OF 1
AD
A036214





NATIONAL BUREAU OF STANDARDS-1963-A

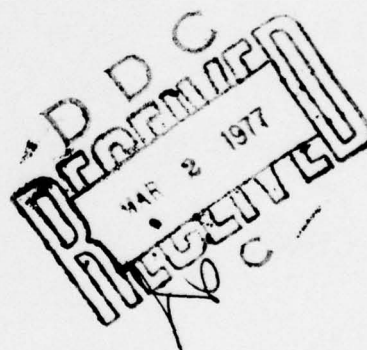
AD A036214

AFAPL-TR-76-105

12
NW

IN-SITU MEASUREMENTS OF GAS SPECIES CONCENTRATIONS IN SIMULATED DUMP COMBUSTOR FLOWFIELDS

WRIGHT STATE UNIVERSITY
DAYTON, OHIO 45431



NOVEMBER 1976

TECHNICAL REPORT AFAPL-TR-76-105
FINAL REPORT FOR THE PERIOD 23 SEPTEMBER 1975 - 30 SEPTEMBER 1976

Approved for public release; distribution unlimited

AIR FORCE AERO PROPULSION LABORATORY
AIR FORCE WRIGHT AERONAUTICAL LABORATORIES
AIR FORCE SYSTEMS COMMAND
WRIGHT-PATTERSON AIR FORCE BASE, OHIO 45433

NOTICE

When Government drawings, specifications, or other data are used for any purpose other than in connection with a definitely related Government procurement operation, the United States Government thereby incurs no responsibility nor any obligation whatsoever; and the fact that the Government may have formulated, furnished, or in any way supplied the said drawings, specifications, or other data, is not to be regarded by implication or otherwise as in any manner licensing the holder or any other person or corporation, or conveying any rights or permission to manufacture, use, or sell any patented invention that may in any way be related thereto.

This report describes a contractual research effort involving the assembly, calibration and operation of an on-line, real-time gas sampling and analysis system. The main component of this system was a quadrupole mass spectrometer. The work was performed by Wright State University, under contract F33615-76-C-2010 in support of Work Unit 70651226. The technical monitor for this contract was Dr. James E. Drewry of the Ramjet Engine Division, Ramjet Technology Branch, Air Force Aero Propulsion Laboratory. This work was completed November 1976.

This report has been reviewed by the Information Office (ASD/OIP) and is releasable to the National Technical Information Service (NTIS). At NTIS, it will be available to the general public, including foreign nations.

This technical report has been reviewed and is approved for publication.

James E. Drewry
JAMES E. DREWRY
Project Engineer

FOR THE COMMANDER:

Frank D. Stull
FRANK D. STULL
Chief, Ramjet Technology Branch
Ramjet Engine Division

AIR FORCE - 4 JANUARY 77 - 150

APPROVED BY	DATE	INITIALS
YES	10/11/76	✓
NO		
UNCLASSIFIED		
JUSTIFICATION		
BY DISTRIBUTION/AVAILABILITY CODES		
A		

UNCLASSIFIED

SECURITY CLASSIFICATION OF THIS PAGE (When Data Entered)

REPORT DOCUMENTATION PAGE		READ INSTRUCTIONS BEFORE COMPLETING FORM
1. REPORT NUMBER AFAPL-TR-76-105 ✓	2. GOVT ACCESSION NO.	3. RECIPIENT'S CATALOG NUMBER 9
4. TITLE (and Subtitle) IN-SITU MEASUREMENTS OF GAS SPECIES CONCENTRATIONS IN SIMULATED DUMP COMBUSTOR FLOWFIELDS.	5. TYPE OF REPORT & PERIOD COVERED Technical Final technical rept. 23 Sep 75-30 Sep 76 ✓	6. PERFORMING ORG. REPORT NUMBER
7. AUTHOR(s) C. Chang, G.D. Sides T. O. Tiernan	8. CONTRACT OR GRANT NUMBER(s) F33615-76-C-2010 new	
9. PERFORMING ORGANIZATION NAME AND ADDRESS Wright State University Dayton, Ohio 45431	10. PROGRAM ELEMENT, PROJECT, TASK AREA & WORK UNIT NUMBERS 7065-12+26	
11. CONTROLLING OFFICE NAME AND ADDRESS Air Force Aero Propulsion Laboratory (RJT) Air Force Wright Aeronautical Laboratories Wright-Patterson AFB, Ohio 45433	12. REPORT DATE November 1976	
14. MONITORING AGENCY NAME & ADDRESS (if different from Controlling Office)	13. NUMBER OF PAGES 66	
	15. SECURITY CLASS. (of this report) Unclassified	
16. DISTRIBUTION STATEMENT (of this Report) Approved for public release; distribution unlimited.		
17. DISTRIBUTION STATEMENT (of the abstract entered in Block 20, if different from Report)		
18. SUPPLEMENTARY NOTES 61102F		
19. KEY WORDS (Continue on reverse side if necessary and identify by block number) mass spectrometry species concentrations gas sampling quadrupole mass spectrometer		
20. ABSTRACT (Continue on reverse side if necessary and identify by block number) A sampling probe-mass spectrometer system was assembled, calibrated and operated for making in-situ measurements of the concentrations of gaseous species in a combustor flow field. A series of tests were conducted in order to determine suitable design parameters for the gas inlet system and to determine the optimum operating conditions for the mass spectrometer. The accuracy of the mass spectrometric technique was verified over a wide range of concentrations through the analysis of gas mixtures with known compositions.		

DD FORM 1 JAN 73 1473

EDITION OF 1 NOV 65 IS OBSOLETE

UNCLASSIFIED

SECURITY CLASSIFICATION OF THIS PAGE (When Data Entered)

388 261

UNCLASSIFIED

SECURITY CLASSIFICATION OF THIS PAGE(When Data Entered)

20. Abstract (continued)

In addition to the development of the gas sampling capability of the system constructed in the present research, this apparatus was interfaced to a computer in order to allow high-speed data acquisition and to facilitate data reduction. After the initial design and development phase, the mass spectrometric sampling system was used on a routine basis for the analysis of gas sampled from a simulated dump combustor flow field. Fuel (argon)/air mixing profiles were obtained for various test configurations and flow field conditions. The results of these tests illustrate the applicability of the gas sampling and analysis system to the in-situ measurement of gas species concentrations in high-pressure, ducted flow fields.

↑

UNCLASSIFIED

SECURITY CLASSIFICATION OF THIS PAGE(When Data Entered)

TABLE OF CONTENTS

SECTION	PAGE
I INTRODUCTION	1
II DESCRIPTION OF THE APPARATUS	3
III DEVELOPMENT PHASE FOR THE GAS SAMPLING AND ANALYSIS SYSTEM	5
1. Mass Spectrometer Installation and Testing	5
2. Gas Inlet System Operation	6
3. Data Acquisition Interface	7
4. Mass Spectrometer Operation for Gas Analysis	10
5. Composition of Air in the Combustion Chamber	12
IV OPERATIONAL GAS SAMPLING AND ANALYSIS	13
1. Description of the Dump Combustor and Gas Sampling System	13
2. Measurements of Argon/Air Mixing Profiles	14
3. Reference Probe Measurements	15
4. Listings of Measured Argon/Air Mixing Profiles Under Various Experimental Conditions	16
5. Test of Ar ⁺ Ion Signal Time Response	18
V SUMMARY	20
REFERENCES	21

LIST OF ILLUSTRATIONS

FIGURE		PAGE
1	Schematic Diagram of the Quadrupole Mass Spectrometer and Gas Inlet System	27
2	Photograph of the Quadrupole Mass Spectrometer and Gas Inlet System	28
3	Mass Spectrum of Ambient Air (Low Sensitivity)	29
4	Mass Spectrum of Ambient Air (High Sensitivity)	30
5	Mass Spectrometer X-Axis Output Versus Ion Mass	31
6	Schematic Diagram of the Mass Spectrometer-Computer Interface System (Hardware Components)	32
7	Schematic Diagram of the Mass Spectrometer-Computer Interface System (Software Components)	33
8	Voltages Measured at Various Terminals of the Interface System Versus Voltages Measured at the Mass Spectrometer	34
9	Time Sequence of Events in the Data Acquisition Process	35
10	Plot of Ion Intensity Ratio Ar^+/N_2^+ Versus the Argon/Nitrogen Mass Flow Ratio	36
11	Plots of Ion Intensity Ratio $\text{O}_2^+/\text{N}_2^+$ Versus Time	37
12	Plots of Ion Intensity Ratio $\text{O}_2^+/\text{N}_2^+$ Versus Source Pressure for Ion Energies ≤ 20 Electron Volts	38
13	Plot of Ion Intensity Ratio $\text{O}_2^+/\text{N}_2^+$ Versus Source Pressure for an Ion Energy of 40 Electron Volts	39
14	Plot of N_2^+ Ion Signal Versus Source Pressure	40
15	Mass Spectrum of Ambient Air	41
16	Mass Spectrum of Compressed Air/Injected Argon	42
17	Schematic Diagram of the Combustor and Gas Sampling System	43
18	Schematic Diagram of the Sampling Probes (A. Impact Probe. B. Static Probe.)	44
19a	Time Profiles of the N^+ and Ar^+ Signals During a Typical Combustor Experiment (No Injected Argon)	45

LIST OF ILLUSTRATIONS (continued)

FIGURE		PAGE
19b	Radial Profiles of the N^+ and Ar^+ Signals During a Typical Combustor Experiment (No Injected Argon)	46
20a	Time Profiles of the N^+ and Ar^+ Signals During a Typical Combustor Experiment (With Injected Argon)	47
20b	Radial Profiles of the N^+ and Ar^+ Signals During a Typical Combustor Experiment (With Injected Argon)	48
21	Mole Fraction of Injected Argon Versus the Radial Position of the Sampling Probe	49
22	Comparison of the Injected Argon/Air Ratios Calculated from Measured Ar^+/N^+ Ratios with Those Calculated from the Measured Argon and Air Mass Flow Rates	50
23a-i	Mole Fraction of Injected Argon Versus the Radial Position of the Sampling Probe (see Table II for the experimental conditions applicable to each figure)	51-59
24	Schematic Diagram of the Flame Holders (4-element Array and 3-element Array)	60
25	Comparison of the Injected Argon Concentration Profiles Obtained With and Without the Flame Holder	61
26	Plots of Argon Ion Signal Time Response for Gas Sampled from the Sampling Probe	62
27	Plots of Argon Ion Signal Time Response for Gas Sampled from the Reference Probe	63

SECTION I

INTRODUCTION

It is well recognized that a thorough understanding of the processes of turbulent mixing, ignition and combustion of gaseous fuels in flow fields, such as those present in a dump combustor,¹ is vital to the successful design and development of advanced air-breathing propulsion systems. A laboratory study of these fluid dynamic and chemical kinetic processes has been conducted for the past few years as part of an in-house Air Force research program.² One of the most difficult problems encountered in these laboratory studies is the accurate determination of the gas composition at various stages of the fuel/air mixing process inside the combustion chamber. The present contractual effort was undertaken for the purpose of developing and assessing a gas analysis method which would be capable of rapid sampling and data acquisition.

The method selected by APL[†] for in-situ gas concentration measurements utilizes a mass spectrometer. The use of a mass spectrometer for gas analysis allows data corresponding to gas concentration to be obtained rapidly. In addition, this instrument may be easily interfaced to a computer so that the data obtained may be reduced to the desired format for display. The disadvantages of a mass spectrometric technique for in-situ gas concentration measurements include the requirement that the pressure of the gas in the combustion chamber (hundreds of torr) be reduced to the pressure limit required by the mass spectrometer for proper operation (less than 10^{-4} torr) and that the apparent concentrations of gaseous species present in the combustion chamber not be altered in the sampling process. These problems can be solved by the proper design of the mass spectrometer gas inlet system.

The mass spectrometer selected by APL for gas analysis is a quadrupole type. This mass spectrometer is widely used for analytical applications.³ It has several desirable features including simplicity of operation, small size, rapid response and peak-switching or mass-scanning modes of operation.

[†] Air Force Aero Propulsion Laboratory

It may also be easily interfaced to computer systems. This is required in the present research since data must generally be obtained at high rates in combustor research.

It should be noted that the purpose of this report is to discuss the implementation of a mass spectrometric technique for the in-situ measurement of gas concentrations in a simulated combustor flow field. Typical data obtained during the current research effort is presented here in order to illustrate the operation of the gas sampling technique. The significance of these data in terms of flow field characterization is not discussed in any detail but has been reported in Ref. 4.

SECTION II

DESCRIPTION OF THE APPARATUS

A schematic illustration of the quadrupole mass spectrometer and gas inlet system is shown in Fig. 1. A photographic view of the gas sampling system is shown in Fig. 2. The gas, whose composition is to be determined, is usually introduced through valve #2. A portion of the sample gas flow enters the prechamber through valve #4. Most of the gas is pumped away through valve #3. Due to the limited pressure range within which the mass spectrometer will operate properly, most of the gas flowing into the prechamber is pumped away through valve #5 by a mechanical pump. Only a small amount of the original gas flow enters the mass spectrometer (through a 0.006 inch orifice) to be analyzed.

The mass spectrometer chamber is pumped by a four-inch oil diffusion pump, which is backed by a mechanical forepump. A cooled trap prevents oil vapor in the diffusion pump from reaching the mass spectrometer chamber. The system has been operated with the trap filled with liquid nitrogen and with the trap filled with ethanol cooled by a refrigerated system. As previously mentioned, the pressure within the mass spectrometer chamber must be maintained at less than 1×10^{-4} torr. A pressure protect system automatically shuts off the mass spectrometer any time the pressure exceeds a preset limit.

As seen in Fig. 1, the mass spectrometer consists of four main components. A detailed description of these components will not be presented here since their operation has been well documented elsewhere.⁵ Briefly, gas molecules are detected by observing the ionic species formed by electron impact in the ionizer. These ions are detected by first extracting them from the ionizer and allowing them to pass through a series of ion lenses. These lenses focus the ions at the entrance of a quadrupole mass filter. Only ions of a specific charge to mass ratio (depending on the values of the DC and RF voltages on the poles) pass through the filter and are detected by the electron multiplier. Data are usually obtained with the mass spectrometer in a scanning mode so that a normal mass spectrum is obtained.

If one is interested in ions of specific masses, then the system can be operated in a peak-switching mode in which up to six ion mass ranges can be scanned sequentially or six individual ion peaks can be observed. In the present argon/air mixing studies, the Ar^+ and N^+ ions were observed in the peak-switching mode of operation. This allows one Ar^+/N^+ ratio measurement to be obtained every two seconds if the scan period for each mass channel is set at one second.

SECTION III

DEVELOPMENT PHASE FOR THE GAS SAMPLING AND ANALYSIS SYSTEM

1. Mass Spectrometer Installation and Testing

The quadrupole mass spectrometer system was assembled and installed in the vacuum housing. All electrical cables to the mass spectrometer from the control units were checked before connection in order to ensure that the correct voltages were being supplied to the mass filter and to associated lens and source elements. The previously assembled vacuum control panel, used to operate valves in the pumping manifold, was also tested. When these preliminary tests were completed, the mass spectrometer housing was evacuated and the system tested for leaks. The system could be pumped down to a residual pressure of less than 2×10^{-7} torr. When an adequate vacuum had been achieved in the system, the quadrupole mass spectrometer controls were adjusted and the mass filter tuned in order to produce mass spectra with the desired resolution and system sensitivity.

In order to introduce gases into the mass spectrometer, it was necessary to design and fabricate a gas inlet system. This is shown schematically in Fig. 1, along with the other components of the gas analysis system. In one configuration of this system, the gas sample is introduced through the probe inlet, which will be described later. For the purpose of testing the mass spectrometer, room air was injected through valve #1. Air spectra were then observed. Typical spectra are shown in Figs. 3 and 4. The electrometer sensitivity (determined by the input resistor) was larger by a factor of 100 for the scan shown in Fig. 4 than for the corresponding scan in Fig. 3. As seen in Fig. 3, the nitrogen ($m/e = 28$) and oxygen ($m/e = 32$) peaks are in the correct ratio for air (assuming that the mass filter gives approximately equal responses for the two gases), indicating that the mass spectrometer is adjusted correctly to minimize mass discrimination effects. The presence of other minor components, such as argon ($m/e = 40$), carbon dioxide ($m/e = 44$) and higher mass trace constituents, is also evident in the spectrum shown in Fig. 4.

After the initial installation and operation of the mass spectrometer, a calibration of the X-axis output (proportional to the mass to charge ratio) versus ion mass was completed for both the low mass and high mass scales. The results of this calibration are shown in Fig. 5. These calibration plots show that the voltage output versus ion mass is quite linear for both the low mass and high mass scales. The coefficients relating the ion mass to voltage output are seen to be 0.015 volts/mass unit and 0.0075 volts/mass unit for the low mass and high mass scales, respectively. These voltage versus ion mass calibration curves have been very stable over the period of time the system has been in operation thus far. The numbers 1.333 and 6.455 in Fig. 5 are potentiometer dial readings on the mass spectrometer control chassis for the low mass and high mass scales, respectively.

2. Gas Inlet System Operation

One of the limitations of the present analytical technique is the requirement that the ion source pressure be lower than 1×10^{-4} torr in order to operate the mass spectrometer. This requirement sets an upper limit on the flow rate of the sample gas into the ion source region of the mass spectrometer. After the installation of the gas inlet system shown in Fig. 1, the pressure in the prechamber and in the mass spectrometer chamber were determined as a function of pressure at the sampling probe entrance. The sampling probe used has a 0.020 inch I.D. opening at its tip. The results of these pressure measurements are shown in Table I. The results for two different configurations between the probe line and the gas inlet system are shown in Table I. As shown in Fig. 1, the probe inlet is usually connected through valve #2. The probe inlet may also be connected to the valve #1 port if valve #1 is replaced with an on-off valve with the same conductance as valve #2. It is interesting to note that the differential pumping efficiency is far greater when the probe inlet is connected through valve #1. Gas may be sampled at a pressure up to 50 psig in this configuration compared to a maximum gas pressure of 30 psig when the probe inlet is connected through valve #2. This difference is probably due to more efficient pumping through valve #3 when the flow of gas is aligned with the direction of the pumping line. It should be noted that

the results shown in Table I do not necessarily reflect conditions during the actual sampling of gas from the combustor chamber since the upper pressure limit which may be sampled also depends on other factors, such as the sampling probe geometry and the flow velocity of the gas mixture in the vicinity of the probe tip inside the combustor chamber.

3. Data Acquisition Interface

Analog signals corresponding to various experimental parameters (ion mass, ion intensity, source pressure) are available at the mass spectrometer. These signals are interfaced to the computer in the manner shown in Figs. 6 and 7. The signals go through two patchboards to amplifiers which increase the signals to 5 volts full scale at the analog-to-digital (A/D) converter.

During the initial testing of the computer interface system, the signals present at the mass spectrometer were traced through cables connecting them to the computer. The voltages at various points in the system were compared to the voltages at the mass spectrometer as shown in Fig. 8. The numbers 5, 6 and 7 correspond to the output of amplifiers with gains 1, 10 and 5, respectively. The numbers 63, 64 and 65 correspond to voltage inputs at the A/D converter. The letters PP and QQ correspond to voltages measured at the patchboard near the mass spectrometer. The measurements shown in Fig. 8 were made after the amplifiers were adjusted for the exact gain desired and for zero offset at the amplifier output (that is, zero signal input yields zero signal output). The results in Fig. 8 show that the hardware between the mass spectrometer and the computer A/D converter functions properly.

It is not necessary to continually adjust the amplifiers to achieve the performance shown in Fig. 8. In fact, this procedure may not be strictly correct since the zero offset and gain parameters of each channel of information may depend on the total effect of each element of hardware (amplifier, connecting cables, patchboards and A/D converter) making up a single channel of information. Thus, before each experiment, a calibration procedure is completed for each information channel. This procedure consists of two steps for each channel. First, the operator adjusts a given

experimental parameter at the mass spectrometer to zero. The computer is told that the value of the experimental parameter corresponding to the channel being calibrated should be zero. The computer may actually receive a non-zero number of counts from the A/D converter because of zero offset in hardware making up the channel under test or because the analog output at the mass spectrometer may not be zero. The operator then adjusts the experimental parameter to a non-zero value. The computer is told the new value (in engineering units) of this experimental parameter. The computer stores the number of counts received from the A/D converter for the channel under test. The calibration is then completed by solving the simultaneous equations

$$0 = K_i (a_i N_{i0} + b_i)$$

$$S_i = K_i (a_i N_{i1} + b_i)$$

where K_i is a constant relating the counts from the A/D converter to the engineering units of the measured experimental parameter, N_{i0} is the number of counts received with the experimental parameter adjusted to zero, N_{i1} is the number of counts received from the A/D converter with the experimental parameter adjusted to the value S_i , a_i and b_i are the calibration constants to be determined, and i refers to the i^{th} channel of information. This calibration process is repeated for each channel connecting the mass spectrometer to the computer.

In addition to monitoring analog signals from the mass spectrometer, the computer receives digital information from the mass programmer unit. This information corresponds to the channel number being monitored by the mass spectrometer at the time the information was taken. This channel number tells which mass or range of masses, as determined by the operator, are being monitored by the mass spectrometer. The channel number is thus a redundant means of determining the ion mass.

The interface system also allows a pulse (5 volts, 10 millisecond duration), which is synchronized with the computer data acquisition process, to be used to control the rate at which the mass spectrometer acquires data. This pulse is input to the sync-in BNC connector at the rear of the mass

programmer. (The relationship of this pulse to the data acquisition process is shown in Fig. 9.) Upon receiving the synchronized pulse, the mass programmer activates a new mass channel and scans that channel at a pre-determined speed. Information is not accepted by the computer until approximately 117 milliseconds after the synchronizing pulse is received. Information is accepted by the computer during the time interval 117 to 1000 milliseconds after the synchronizing pulse. Therefore, the mass spectrometer is adjusted so that the desired information falls within this time interval. During this period, there are a total of 128 samples collected and averaged to yield a value representing the integrated peak area. The integration reduces the effect of 60 Hertz noise in the transmission lines between the mass spectrometer and the computer and reduces the effect of drift in the location of the window being observed in the ion signal versus mass spectrum.

The data acquisition cycle described above yields the area of one ion peak each second. Since meaningful information can be obtained only by comparing the sample ion intensity (Ar^+) with the reference ion intensity (N^+), two seconds are required for each data point. Although this data acquisition rate is usually sufficient, it may be desired to sample at higher speeds, especially if reactive flows are sampled. Therefore, a high-speed integration program was developed. This program allows up to 10 peak integrations per second. Thus, the time required to obtain each data point (Ar^+/N^+ ratio) is reduced to only 0.2 seconds. It should be noted, however, that this increase in the data acquisition rate is achieved at the expense of integration accuracy. Each integrated peak is the average of only eight samples as opposed to 128 samples used in the low-speed integration mode. The obvious advantage of the high-speed integration mode is that a larger number of data points may be obtained for a given experimental event. However, the high-speed integration mode does present a data handling and storage problem due to the large number of data points obtained. This method was not used on a routine basis but will probably be used extensively in the future for combustion experiments where high-speed data acquisition is necessary.

4. Mass Spectrometer Operation for Gas Analysis

In the present fuel (argon)/air mixing studies, the argon/air concentration ratio in a simulated dump combustor flow field was obtained by comparing the measured Ar^+/N^+ ion intensity with the Ar^+/N^+ ratio obtained from air for which the argon/nitrogen ratio is known. This technique requires that the relationship between the measured ion intensity ratios and the gas concentration ratios, within the concentration range of interest, be linear. This assumption of linearity was tested before the technique mentioned above was applied to the analysis of any unknown gas mixtures.

The test mentioned above was performed by making up a series of argon/air mixtures of known composition and measuring the Ar^+/N^+ ratios for each mixture. These Ar^+/N^+ ratios were measured under the same conditions as a typical experiment during which gas is sampled from the combustor chamber (~ 3 torr pressure in the prechamber, $\sim 10^{-5}$ torr in the mass spectrometer chamber and with valves #3 and #5, shown in Fig. 1, fully open). The results of these tests, shown in Fig. 10, indicate that the requirement of linearity is fulfilled within the range of argon/nitrogen ratios used in the present research, and that the analytical technique developed in the present research is correct.

In a typical combustor experiment gas is sampled and analyzed continuously for a period of thirty minutes or more. Thus, it is necessary that the monitored ion intensity ratio remain constant within this period for a fixed gas composition. There is generally no difficulty in meeting this requirement under normal operating conditions, that is, when the mass spectrometer source pressure is on the order of 10^{-6} torr. However, the sampling of gas from the combustor produces an operating pressure in the source of 10^{-5} torr or higher. At this high source pressure, space charge effects within the source may cause large fluctuations in the ion signals observed. This problem may be eliminated through the adjustment of mass spectrometer operating parameters.

The ion signal stability was tested by monitoring the intensities of O_2^+ and N_2^+ ions as a function of time with a high pressure (1×10^{-5} torr)

of air in the ion source. The high source pressure was obtained by opening valve #1 (see Fig. 1) and raising the pressure in the prechamber until the source was at the desired pressure. The results of one set of measurements are shown in Fig. 11. It was discovered that the stability of the O_2^+/N_2^+ ratio was very dependent on the value of the ion energy (the energy of the ions entering the quadrupole region of the mass spectrometer). This result is not unexpected since the high density of ions in the source means that space charge effects will be significant and will be an important influence on the trajectory of low energy ions. As the ion energy was increased from 20 to 40 electron volts, it was observed that the ion signals O_2^+ and N_2^+ increased drastically. This indicates that space charge effects are significant at low ion energies. At an ion energy of 40 electron volts the O_2^+/N_2^+ ratio was found to be stable over a 40 minute time period to within $\pm 0.1\%$. Therefore, all experiments were performed at ion energies ≥ 40 electron volts.

In addition to the requirement that ion signal ratios such as O_2^+/N_2^+ be independent of time, it is also desirable that these ratios not vary significantly with small source pressure fluctuations ($\sim \pm 10\%$) since there may be local pressure variations in the combustion chamber during an actual experiment. Figure 12 shows plots of O_2^+/N_2^+ ratios versus source pressure for various ion energies < 20 electron volts. It was found that the O_2^+/N_2^+ ratios varied significantly with source pressure. Any attempt at quantifying the change in these ratios for a given change in pressure in the source was also impeded by the time instability of these ratios for low ion energies, as shown by the scatter in the data taken at different times. Figure 13 illustrates the good stability of the O_2^+/N_2^+ ratio versus source pressure when the ion energy is adjusted to 40 electron volts. For a source pressure change from $\sim 2 \times 10^{-5}$ to $\sim 10 \times 10^{-5}$, the O_2^+/N_2^+ ratio changes by only $\sim 5\%$. The pressure stability of the O_2^+/N_2^+ ratio indicates also that the ion energy should be ≥ 40 electron volts.

Figure 14 is a plot of the N_2^+ signal from the mass spectrometer versus source pressure at an ion energy of 40 electron volts. The non-linearity observed is probably due to space charge effects.

5. Composition of Air in the Combustion Chamber

In order to make sure that there were no significant impurities in the test air and injected argon used in the dump combustor experiments, a spectrum of room air (Fig. 15) was compared to a spectrum of compressed air with ~ 4.4% added argon (Fig. 16) used in the combustor. Both spectra are normalized to the O_2^+ peak. There are no significant differences in the two spectra with the exceptions of the O^+ peak and the m/e 29 peak which are larger in room air than in the compressed air. Thus, there are no significant impurities in the gas used in the combustor.

SECTION IV
OPERATIONAL GAS SAMPLING AND ANALYSIS

1. Description of the Dump Combustor and Gas Sampling System

After the completion of the preliminary work described thus far in this report, the technique under development was used to analyze gas sampled in non-reactive combustor experiments. Figure 17 shows a schematic diagram of the dump combustor geometry and gas sampling system. Air is introduced into the combustor at a total pressure of 2-3 atmospheres and at a flow Mach number of approximately 0.7. The trace gas, argon, is injected into the air flow through a total of eight ports as shown in Fig. 17. Each port has an orifice diameter of 0.035 inch. In this configuration, the argon flow through these orifices is choked if the upstream pressure of argon (P_{of}) is maintained at a sufficiently high value. The argon is supplied by two cylinders of pure argon. The pressure, P_{of} , and thus, the argon flow rate, is controlled by two-stage pressure regulators. The degree of mixing within the combustor duct is determined by sampling the gas at various axial and radial locations, with the sampling probe, as shown in Fig. 17. The sampled gas is analyzed on-line and in real-time with the mass spectrometer system. In the present experimental configuration, the sampling probe may be located at six different axial positions within the combustor. The sampling probe is also equipped with an electromechanical drive (not shown in Fig. 17) which moves the probe across the mixing zone at a constant speed, either forward or backward, over a total traversing distance of approximately 3.4 inches. This allows the radial gas concentration profile for injected argon to be obtained at any of the six axial locations of the sampling probe.

In the present experiment, two types of sampling probes (shown in Fig. 18) were used to sample gas in the combustor. The first type is a static pressure probe which has four orthogonal openings on its side, the diameter of each being approximately 0.010 inch. The second type is an impact sampling probe with an orifice diameter of 0.020 inch. The total sampling area of each probe is identical. However, since the impact sampling probe is directed against the flow of the argon/air mixture in the combustor,

it will sense the total pressure field in the vicinity of the probe tip. On the other hand, the static pressure probe will sense only the static pressure field within the combustor. As a result, far more gas can be collected with the impact sampling probe than with the static pressure probe. This is verified by the fact that the impact sampling probe yields a much higher ion source pressure than the static sampling probe under identical experimental conditions.

2. Measurements of Argon/Air Mixing Profiles

In order to determine argon concentrations from measured Ar^+/N^+ ratios, the Ar^+/N^+ ratio is first measured for the known mixture, air, in the combustion chamber. The concentrations of argon and nitrogen in the atmosphere are 0.934% and 78.03%, respectively. The Ar^+/N^+ ratio is then measured under the same experimental conditions for the injected argon/air mixture in the combustion chamber. The mole fraction of injected argon (defined as the moles per unit volume of injected argon divided by the moles per unit volume of air) in the injected argon/air mixture may be written in terms of the measured Ar^+/N^+ ratios.

$$\text{MF} = 0.00934 \left[\frac{(\text{Ar}^+/\text{N}^+)_{\text{mix}}}{(\text{Ar}^+/\text{N}^+)_{\text{air}}} - 1 \right]$$

where MF is the mole fraction of the injected argon in the mixture.

Figures 19 and 20 show typical radial (time) profiles of N^+ and Ar^+ ion intensities for gas sampled by a sampling probe and analyzed using the mass spectrometer system. These profiles were obtained by monitoring Ar^+ and N^+ as the sampling probe traversed the combustor at a constant rate. Figures 19a and 19b show that the absolute intensities of both the N^+ and Ar^+ ions vary with the radial position of the probe in the combustion chamber. The Ar^+/N^+ ratio also varies slightly as the radial position of the probe changes. This effect is due to the radial dependence of the pressure of air in the combustor. Regardless of this variation of the Ar^+/N^+ ratio, the argon concentration in air is constant. In order to allow for the variation of the measured Ar^+/N^+ ratio in air as a function of radial

position, the $(\text{Ar}^+/\text{N}^+)_{\text{air}}$ and $(\text{Ar}^+/\text{N}^+)_{\text{mix}}$ ratios must be measured at the same radial probe position.

Figure 21 is a plot of the mole fraction of injected argon as a function of the radial position of the probe. This plot is obtained by analyzing the raw data shown in Figs. 19 and 20. The mixing profile obtained is symmetric with respect to the combustor centerline ($Y = 1.92$ inches), as expected, since the argon injection rate is the same at all eight injection ports. At the centerline, the measured injected argon mole fraction is practically zero, indicating that mixing is far from complete. As will be discussed in a later section, this mixing profile is largely dependent on experimental parameters such as chamber pressure, argon injection rate, nozzle diameter, as well as the axial distance, X , from the sudden-expansion step at the combustor inlet.

3. Reference Probe Measurements

As shown in Fig. 17, a second probe (reference probe) is located at the end of the combustor mixing zone. The tip of this reference probe is fixed at the centerline of the combustor immediately downstream of a nozzle through which the mixed gas flows into the exhaust region. The argon concentration for the gas measured by this probe represents the average argon concentration if a homogeneous mixture of injected argon and air is obtained by the time the gas reaches the end of the combustor mixing zone.

The mole fractions calculated from measured Ar^+/N^+ ratios can be compared with mole fractions calculated from known mass flow rates measured for air and argon. Such a comparison is shown in Fig. 22. Data points located on the solid line indicate complete agreement between mole fractions calculated from Ar^+/N^+ ratios and those calculated from measured mass flow rates. The agreement is near perfect for the lowest combustor pressure at both injection rates but becomes poorer as the combustor pressure is increased. This may indicate incomplete mixing at high combustor pressures. One other possible explanation for the discrepancy is that the calculation of argon mass flow rates at high chamber pressures is subject to error due to the fact that flow through the injection orifice may not be choked.

4. Listings of Measured Argon/Air Mixing Profiles Under Various Experimental Conditions

A complete listing of the measured argon/air mixing profiles obtained in the present research is given in Table II. These profiles were obtained at various values of the following five parameters:

- 1) nozzle orifice size (D^*)
- 2) type of sampling probe
- 3) inlet air pressure (P_{oa})
- 4) fuel (argon) pressure (P_{of})
- 5) axial distance from combustor inlet (X)

Due to the large volume of data obtained, only a few representative profiles will be presented here in order to demonstrate the effect of the five parameters listed above on the measured mixing profiles. As stated earlier, the purpose of illustrating these data is not to analyze the flow field or mixing mechanism inside the combustor but merely to more clearly demonstrate the capability of the present mass spectrometer technique as a diagnostic tool in analyzing the composition of gas in the combustor for various experimental conditions.

The first parameter to be considered is the effect of the axial distance, X , on the degree of mixing. Figures 23a and 23b clearly demonstrate the change in the radial mixing profile as a function of axial location in the combustor duct.

Apparently, the argon injection rate also has an important effect upon the degree of mixing. Under the present experimental arrangement, an increase in the argon injection rate is achieved by increasing the injection pressure, P_{of} . It is expected that the penetration of the injected argon into the high velocity air flow would increase as the injection pressure increases. This would result in an improvement in the argon/air mixing. Figures 23c and 23d confirm this expectation.

The effect of the combustor static pressure on the mixing is opposite to that of the argon injection pressure, P_{of} . An increase in the static air pressure will effectively resist the penetration of the argon injected

into the chamber and result in poorer mixing. This effect can be seen in Figs. 23e and 23f.

A comparison of the mixing profiles obtained with the impact probe and the static probe may be made from Figs. 23g and 23h. These two figures are essentially identical. This is expected since the true argon composition should not be affected by the amount of sample gas collected.

Figure 23i illustrates a mixing profile obtained with the high-speed integration data acquisition mode for experimental conditions identical to those for the profile shown in Fig. 23h where the low-speed integration mode was used. As seen in these two figures, the mixing profiles are practically indistinguishable.

Near the end of the present research effort, emphasis was shifted to the study of the improvement of fuel (argon)/air mixing through the use of a flame holder which is installed immediately before the sudden expansion region of the combustor. Figure 24 shows the cross sectional view of two types of flame holders tested in the present study. The first type consists of a set of four identical blockage elements with one end of each attached to the flame holder ring and the other end extended into the flow field. As shown in the figure, the cross section of each element is an equilateral triangle with one ridge facing the gas flow. The blockage area of this flame holder is 25% of the total inlet flow area (that is, πR_I^2 in Fig. 24). The second type of flame holder (also shown in Fig. 24) has three identical blockage elements, each 120 degrees from the other. The total inlet blockage is also 25% of the total inlet flow area.

A complete listing of the measured argon/air mixing profiles using a flame holder is included in Table III. One typical profile, illustrated in Fig. 25, clearly shows an improvement in argon/air mixing due to the flame holder. A detailed account of the mixing mechanism is beyond the scope of this report but will be presented elsewhere.⁶

5. Test of Ar^+ Ion Signal Time Response

In the present work, the analysis of argon concentration profiles was achieved by allowing gas in the combustor to flow through metal tubing into the mass spectrometer detection system. Obviously, it requires some finite amount of time for the argon gas to travel the distance starting from the injection port, down the mixing zone (varied from 1-12 inches), and through the entire length of the probe line (~ 10 ft) before it can finally be detected. It is of some interest to determine experimentally the time delay between the injection of argon and the first appearance of the argon ion signal. The information derived from this type experiment should also provide some indication of the feasibility of the present sampling technique in monitoring changes in gas composition during a combustion cycle including fuel injection, ignition, combustion, expansion and exhaust of the burned gas.

Under the present experimental arrangement the injection of argon into the combustor flow field is controlled by a manually operated relay switch which opens the argon injection port valve when the switch is turned on. The probed gas is continuously flowing into the mass spectrometer which is used to monitor argon. The Ar^+ ion intensity is constantly monitored, and this signal serves as the Y-axis input of a X-Y recorder. The X-axis of the recorder is driven by a saw tooth sweep signal. The beginning of the sweep is simultaneous with the opening of the argon injection port relay switch such that the start of the X-Y recorder trace represents the onset of the injection of argon into the combustor flow field.

Figure 26 shows the X-Y recorder traces of the Ar^+ ion signal obtained as a function of time (for both $P_{\text{of}} = 89$ psia and 129 psia) with the time zero representing the opening of the argon injection valve. The gas is sampled through the sampling probe whose tip is located along the centerline, with $X = 2.88$ inches. As seen in the figure, after opening the argon injection valve, the Ar^+ ion signal remains at the background level for approximately 0.2 second. After this initial delay, the signal increases nearly linearly until a constant ion signal is obtained. This signal corresponds to the new gas composition in the flow field. Several seconds after the signal

stabilizes, the argon solenoid valve is closed. This point in time is shown by the arrow in the figure. Again the Ar^+ ion signal remains unchanged for approximately 0.5 second before it decays back to the original level. Figure 27 shows similar data except that gas is sampled from the reference probe.

It should be noted that the apparent Ar^+ ion signal response is affected by the frequency response of the detection system. For example, a test of the X-Y recorder used in these measurements shows that approximately 45% of the Ar^+ ion signal response times shown in Figs. 26 and 27 are simply due to the slow response of the X-Y recorder. Thus, the total response times shown in these figures can only be treated as upper limits of the time delay between the opening (or closing) of the argon injection valve and the detection of this event by the mass spectrometer detection system.

SECTION V

SUMMARY

The results of the present research indicate that non-reactive, simulated fuel-air mixtures at pressures up to several atmospheres can be sampled and analyzed in-situ and in real time using mass spectrometric techniques. This capability enables researchers, investigating high-pressure, high-velocity, non-reactive flow fields, to gather experimental data rapidly and therefore, to study events with greater resolution than was previously possible. This experimental capability will be especially important if the technology developed can be modified and applied to the study of reactive flow fields. Researchers will then have an important diagnostic tool for the study of combustion processes, whether those processes take place in ramjet engines or combustion chambers.

The real-time gas analysis technique developed in the present research has been applied extensively to the investigation of non-reactive flow fields. Much of the experimental data obtained during the course of this study is summarized in the present report. The investigation of non-reactive flow fields was a logical first step in the development of a technique to be used as a diagnostic tool in the study of combustion processes since the difficult problem of designing high temperature probes was avoided. The design of these probes is the modification of the present technique which must be accomplished before the mass spectrometric sampling system can be applied to the study of reactive flow fields. The main problem to be solved is that the probe and gas inlet system must be designed to quench the chemical reaction (combustion process) immediately upon sampling. This problem can be approached now that the analytical technique for non-reactive flow fields has been shown to be operational.

REFERENCES

1. Stull, F.D., Craig, R.R. and Hojnacki, J.J., "Dump Combustor Parametric Investigations," AFAPL-TR-74-90, Air Force Aero Propulsion Laboratory, November 1974.
2. Drewry, J.E., "Supersonic Mixing and Combustion of Coaxial Hydrogen-Air Streams in a Duct," ARL 71-0286, Aerospace Research Laboratories, December 1971.
3. Brubaker, W.M. and Tuul, J., Rev. Sci. Instr., 35 1007 (1964).
4. Drewry, J.E., "Characterization of Sudden-Expansion Dump Combustor Flowfields," AFAPL-TR-76-52, Air Force Aero Propulsion Laboratory, July 1976.
5. Paul, W. and Steinwedel, H. Z. Naturforsch., 8a, 448 (1953); For brief description see any standard textbook, for example, J. Roboz, "Introduction to Mass Spectrometry," (John Wiley & Sons, Inc., New York, N.Y., 1968), Chapter 3.
6. Drewry, J.E., "Fluid Dynamic Characterization of Sudden-Expansion Ramjet Combustor Flowfields," AIAA Paper No. 77-203, AIAA 15th Aerospace Sciences Meeting, Los Angeles, California, January 1977.

TABLE I

MASS SPECTROMETER CHAMBER PRESSURE VERSUS
PRESSURE AT THE REFERENCE PROBE TIP

Probe Site (Valve #)	Pressure at Probe Tip (psig)	Prechamber Pressure (torr)	Mass Spectrometer Chamber Pressure (torr)
1	10	0.7	1.7×10^{-5}
	20	1.4	3.7×10^{-5}
	30	2.0	5.6×10^{-5}
	40	2.7	7.7×10^{-5}
	50	3.3	9.9×10^{-5}
2	5	1.2	3.2×10^{-5}
	10	1.6	4.3×10^{-5}
	15	2.0	5.6×10^{-5}
	20	2.5	7.0×10^{-5}
	25	2.9	8.5×10^{-5}
	30	3.4	1.0×10^{-4}

TABLE II
LIST OF MEASURED ARGON/AIR MIXING PROFILES

Nozzle Orifice I.D. (in.)	Probe	p_{oa}^a (psia)	p_{of}^b (psia)	x^c (in.)	Comment
2	static	22.5	42	1.15	
2	static	22.5	42	2.68	Figs. 23h and 23i
2	static	22.5	42	4.06	
2	static	22.5	42	5.43	
2	static	22.5	42	8.68	
2	static	22.5	42	11.43	
2	static	30.5	42	1.15	Fig. 23a
2	static	30.5	42	4.06	
2	static	30.5	42	5.43	
2	static	30.5	42	11.43	Fig. 23b
2	impact	22.5	42	2.84	
2	impact	22.5	42	8.84	Fig. 23g
2	impact	22.5	42	11.63	
2	impact	30.6	42	5.63	Figs. 19-21
2 1/2	impact	22.5	42	2.87	
2 1/2	impact	22.5	42	8.87	Fig. 23e
2 1/2	impact	22.5	42	11.63	
2 1/2	impact	35.5	46	2.87	Fig. 23f
2 1/2	impact	35.5	46	8.87	
2 1/2	impact	35.5	46	11.63	
2 1/2	impact	49.5	54	8.87	
2 1/2	impact	49.5	54	11.63	
2 1/2	static	22.5	42	8.68	
2 1/2	static	22.5	42	2.68	
2 1/2	static	35.5	46	8.68	
2 1/2	static	35.5	46	2.68	
2 1/2	static	49.5	54	8.68	
2 1/2	static	49.5	54	2.68	
3	static	30.5	43	5.43	
3	static	30.5	87	5.43	Fig. 23d

TABLE II (continued)

Nozzle Orifice I.D. (in.)	Probe	P_{oa}^a (psia)	P_{of}^b (psia)	x^c (in.)	Comment
3	static	30.5	43	11.43	
3	static	30.5	87	11.43	
3	impact	30.5	44	2.87	
3	impact	30.5	87	2.87	
3	impact	30.5	44	8.87	
3	impact	30.5	87	8.87	
2 1/2	impact	30.5	43	2.88	
2 1/2	impact	30.5	86	2.88	
2 1/2	impact	30.5	44	8.88	
2 1/2	impact	30.5	86	8.88	
2 1/2	impact	30.5	44	11.63	
2 1/2	impact	30.5	87	11.63	
2 1/2	impact	30.5	44	5.63	
2 1/2	impact	30.5	87	5.63	
2 1/2	impact	30.5	44	4.25	
2 1/2	impact	30.5	87	4.25	
2 1/2	impact	30.5	44	10.25	
2 1/2	impact	30.5	86	10.25	
2 1/2	static	30.5	86	4.05	
2 1/2	static	30.5	128	4.05	
2 1/2	static	30.5	87	10.05	
2 1/2	static	30.5	129	10.05	
2 1/2	static	30.5	85	8.68	
2 1/2	static	30.5	127	8.68	
2 1/2	static	30.5	87	2.68	
2 1/2	static	30.5	127	2.68	

^aPressure of air.

^bPressure of fuel (simulated by argon)

^cAxial distance of the probe from the combustor inlet.

TABLE III

LISTING OF MEASURED ARGON/AIR MIXING PROFILES^a WITH A FLAME HOLDER

Flame Holder Position	P _{oa} (psia)	P _{of} (psia)	X (in.)	Comment
b	30.5	87	2.68	Fig. 25
b	30.5	87	5.43	
b	30.5	87	8.68	
b	30.5	87	11.43	
b	30.5	129	2.68	
b	30.5	129	5.43	
b	30.5	129	8.68	
b	30.5	129	11.43	
c	30.5	87	2.68	
c	30.5	87	5.43	
c	30.5	87	8.68	
c	30.5	87	11.43	
c	30.5	129	2.68	
c	30.5	129	5.43	
c	30.5	129	8.68	
c	30.5	129	11.43	
d	30.5	89	2.68	
d	30.5	89	5.43	
d	30.5	89	8.68	
d	30.5	89	11.43	
d	30.5	129	2.68	
d	30.5	129	5.43	
d	30.5	129	8.68	
d	30.5	129	11.43	
e	30.5	89	2.68	
e	30.5	89	5.43	
e	30.5	89	8.68	
e	30.5	89	11.43	
e	30.5	129	2.68	
e	30.5	129	5.43	

TABLE III (continued)

Flame Holder Position	P _{oa} (psia)	P _{of} (psia)	X (in.)	Comment
e	30.5	129	8.68	
e	30.5	129	11.43	
e	37	89	2.68	
e	37	89	5.43	
e	37	89	8.68	
e	37	89	11.43	

^aAll data were obtained using the static sampling probe.

^b4-element array positioned in a shape of "X".

^c4-element array positioned in a shape of "+".

^d3-element array positioned in a shape of "inverted Y".

^e3-element array positioned in a shape of "Y".

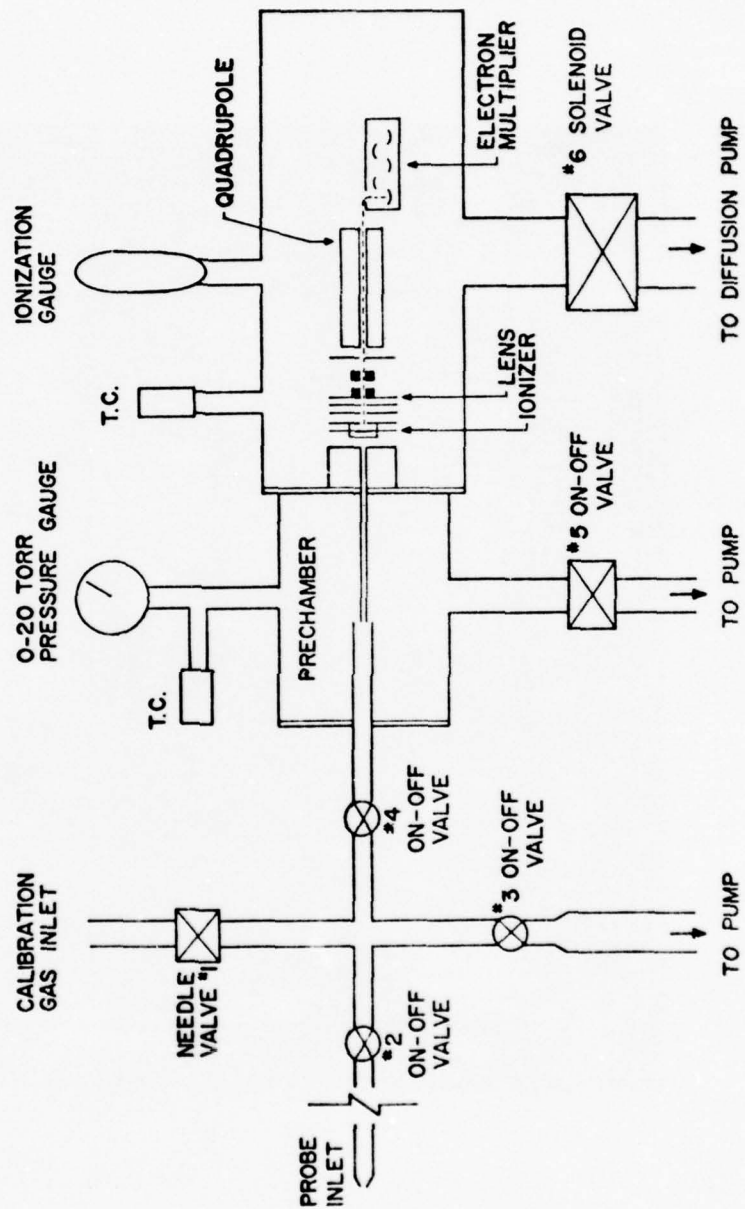


Fig. 1. Schematic Diagram of the Quadrupole Mass Spectrometer and Gas Inlet System

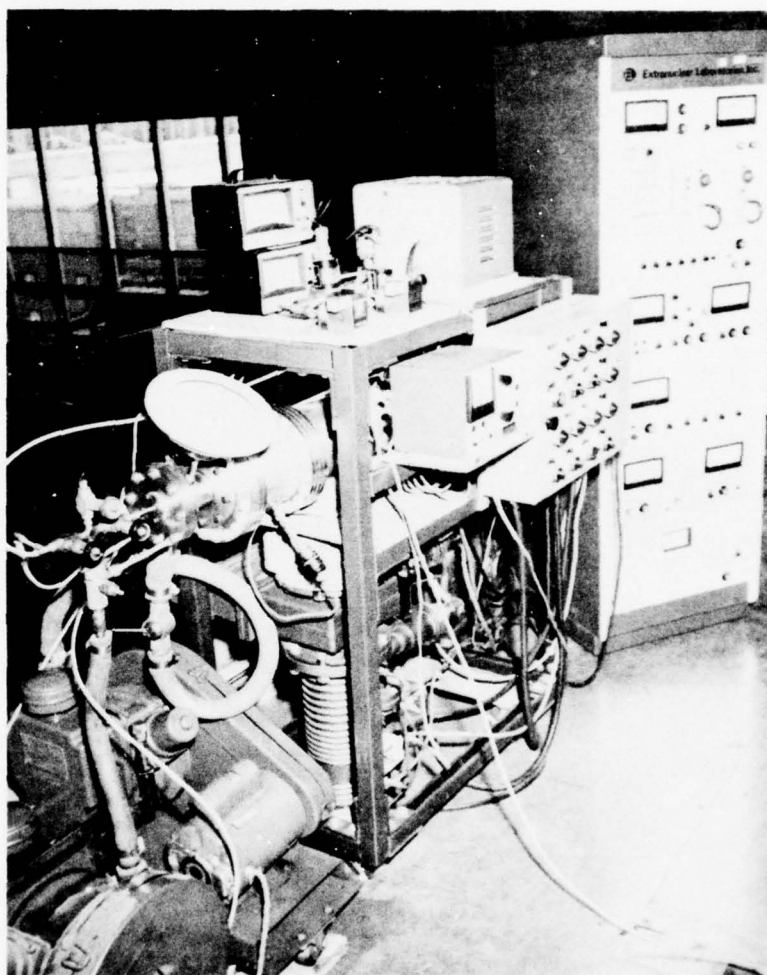


Fig. 2. Photograph of the Quadrupole Mass Spectrometer
and Gas Inlet System

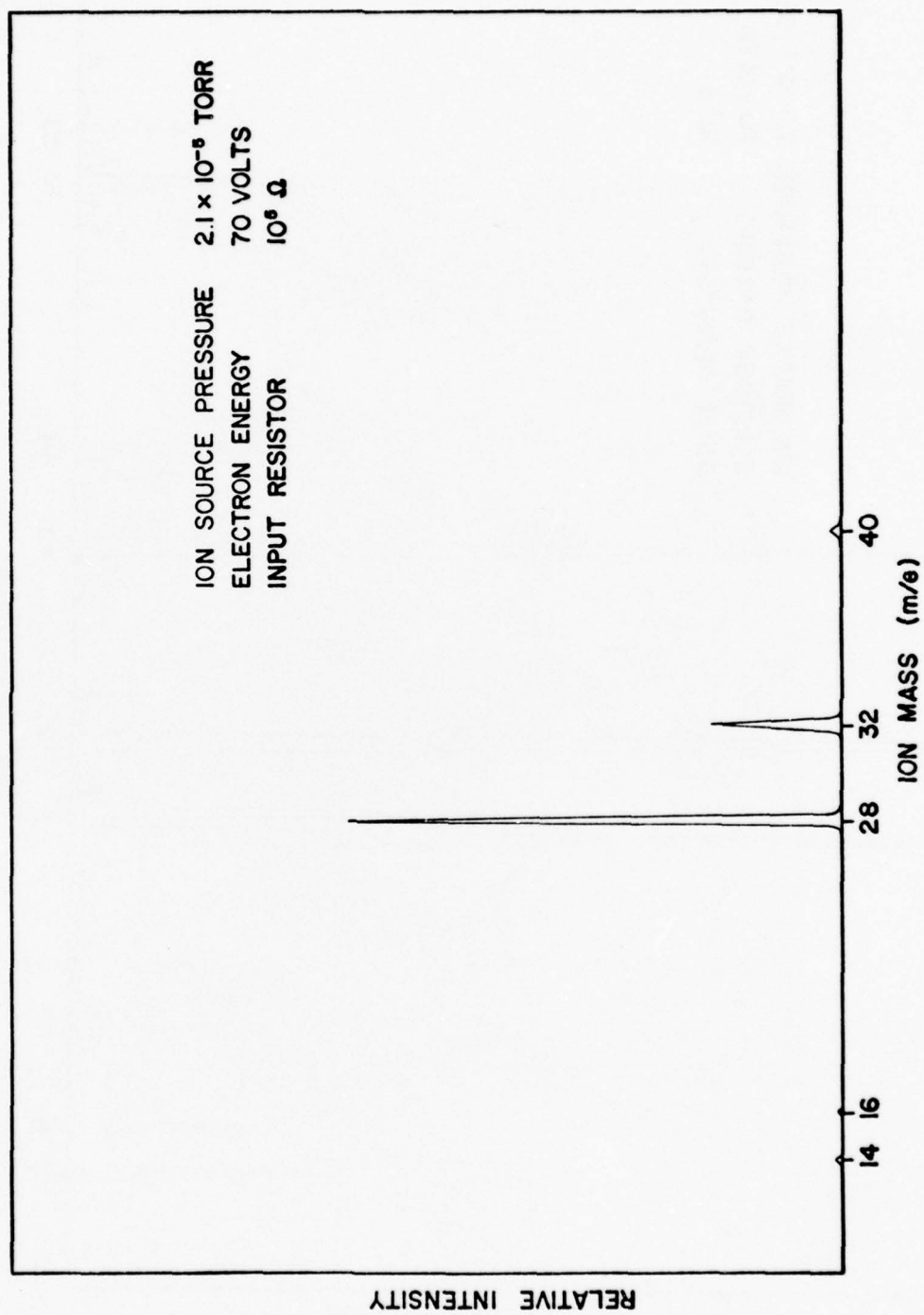


Fig. 3. Mass Spectrum of Ambient Air (Low Sensitivity)

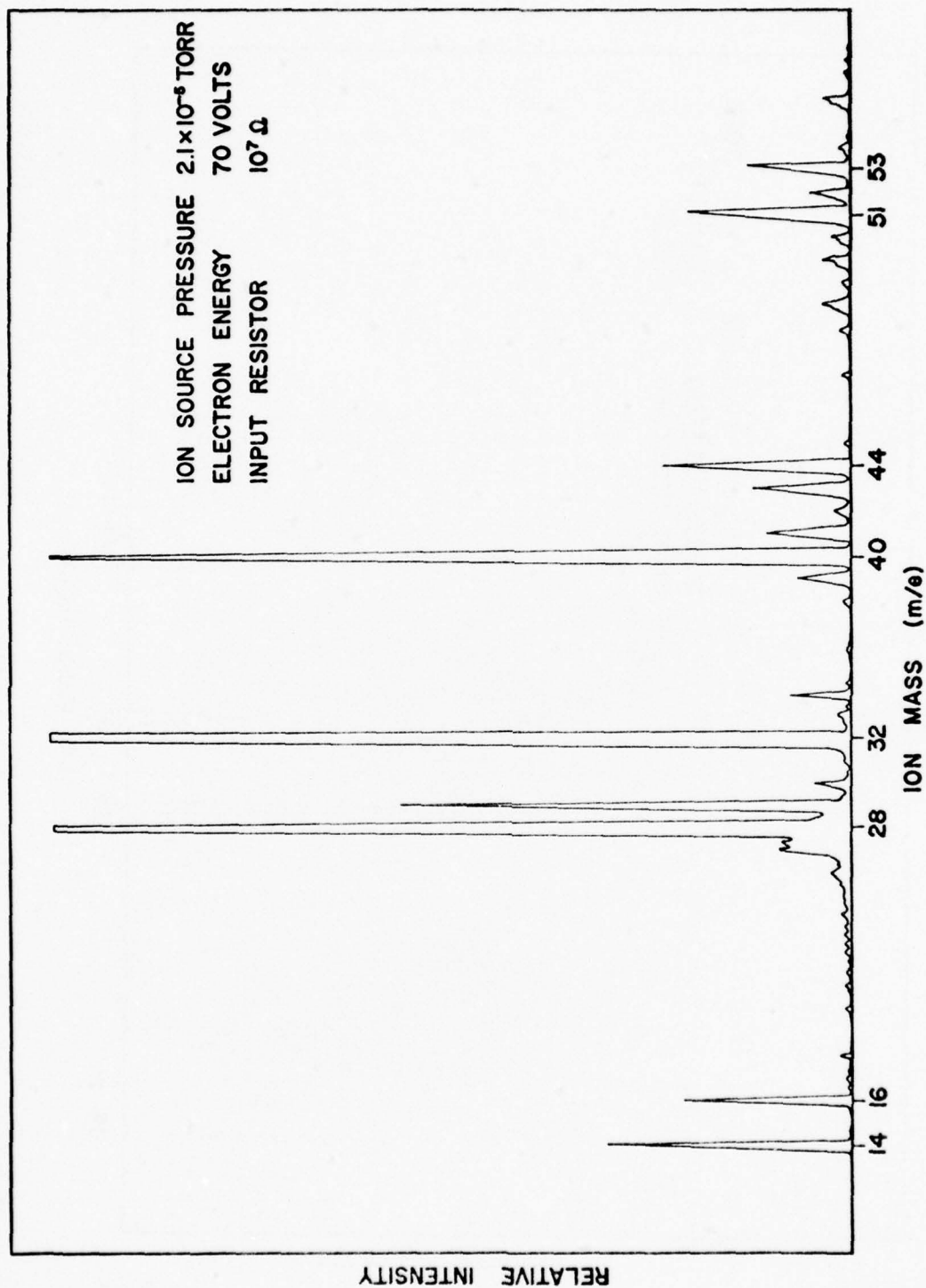


Fig. 4. Mass Spectrum of Ambient Air (High Sensitivity)

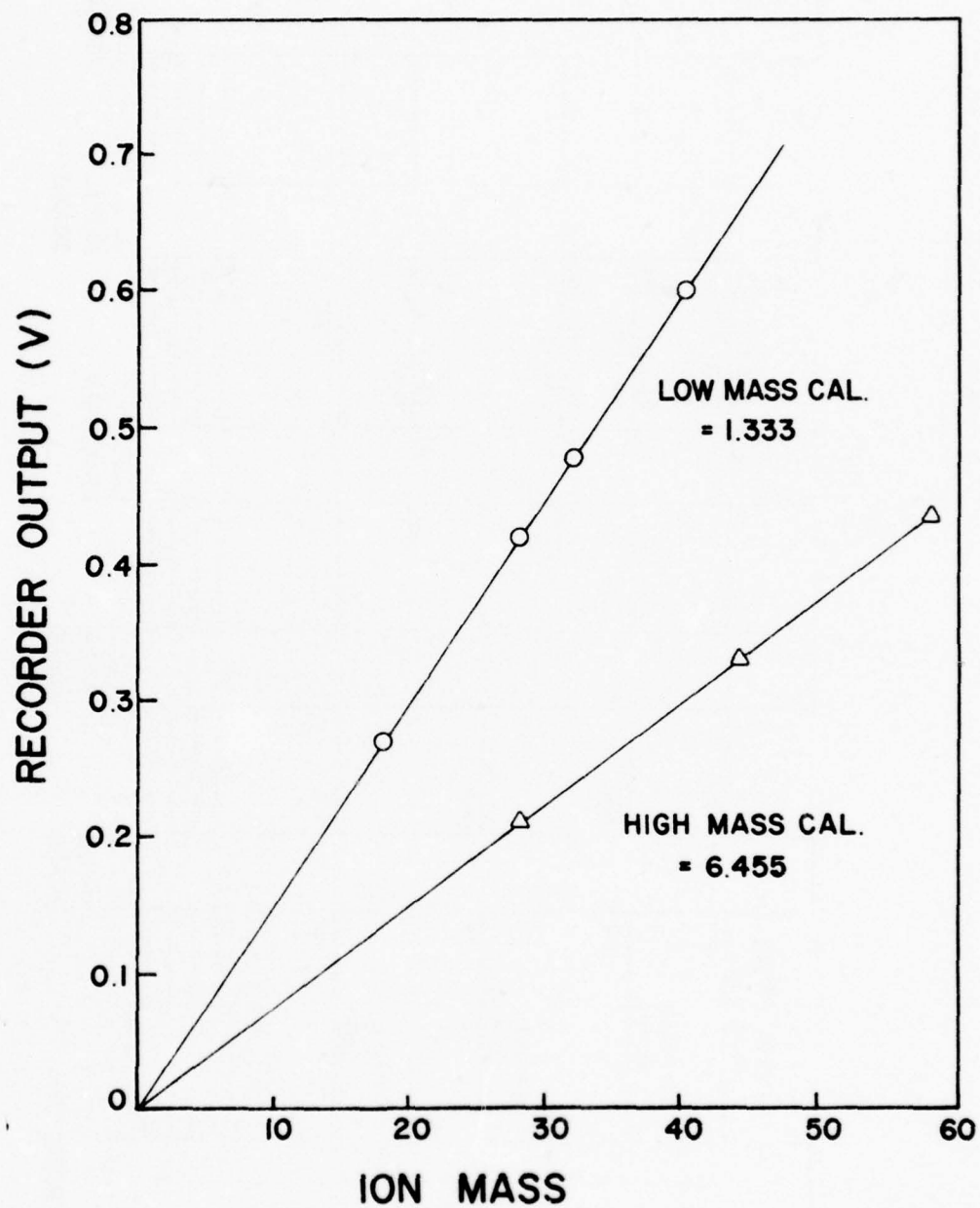


Fig. 5. Mass Spectrometer X-Axis Output Versus Ion Mass

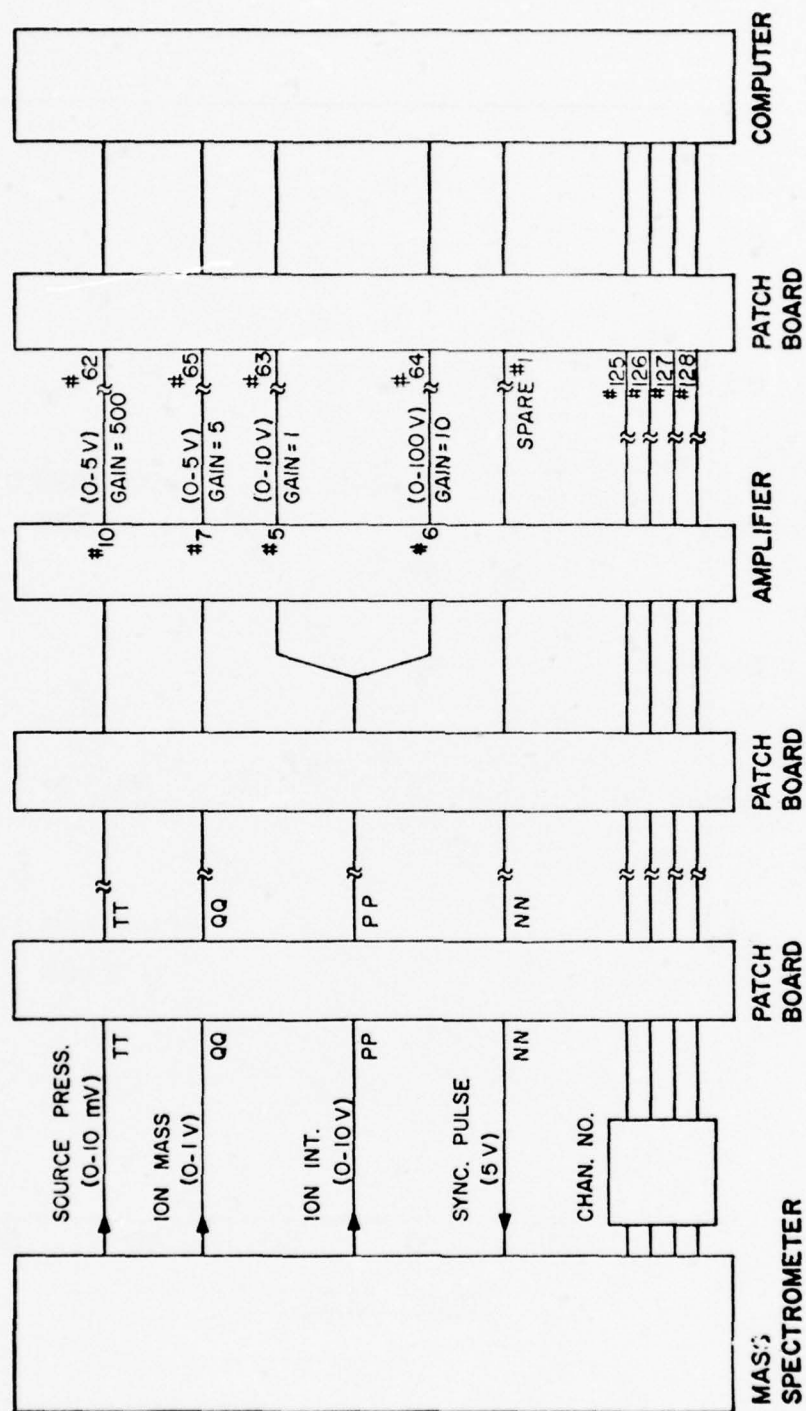


Fig. 6. Schematic Diagram of the Mass Spectrometer-Computer Interface System (Hardware Components)

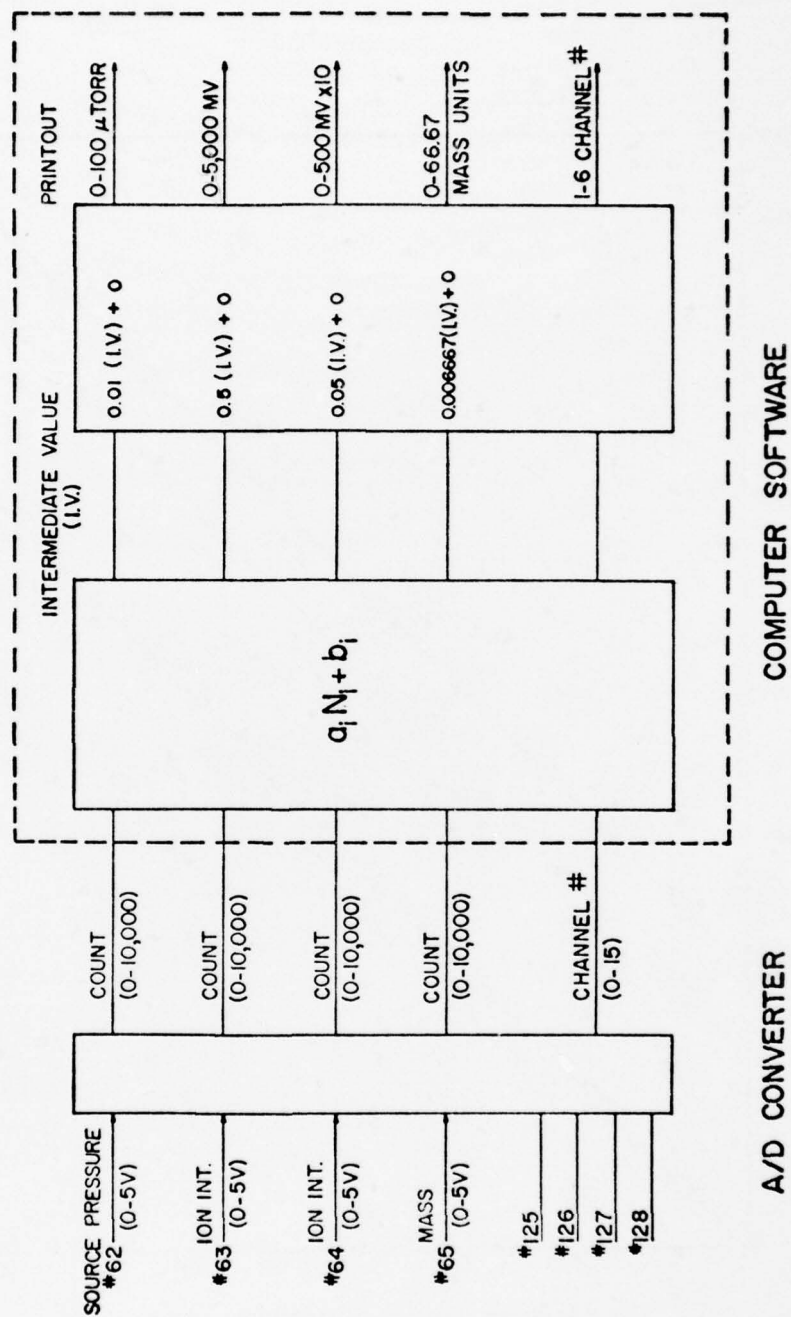


Fig. 7. Schematic Diagram of the Mass Spectrometer-Computer Interface System (Software Components)

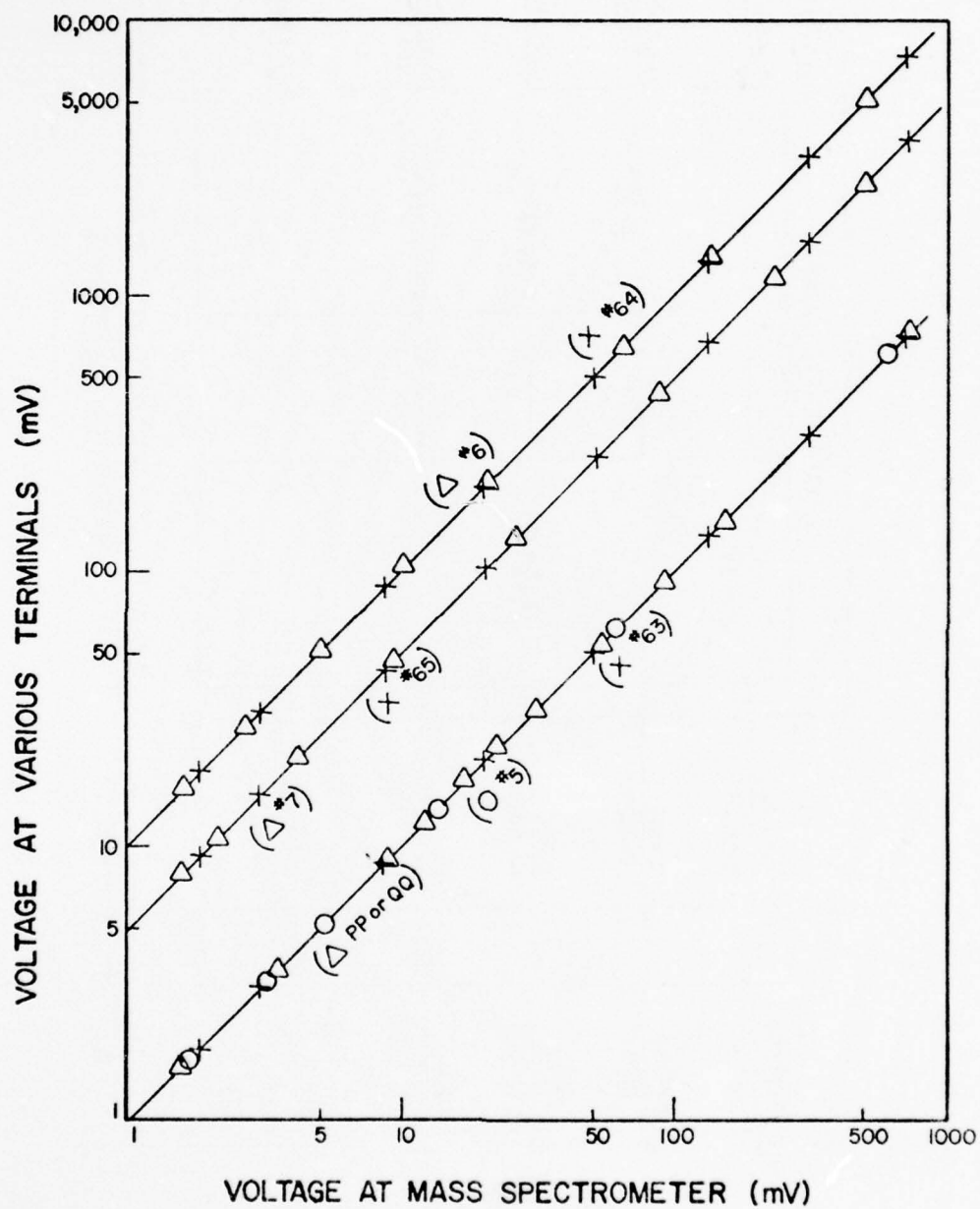


Fig. 8. Voltages Measured at Various Terminals of the Interface System Versus Voltages Measured at the Mass Spectrometer

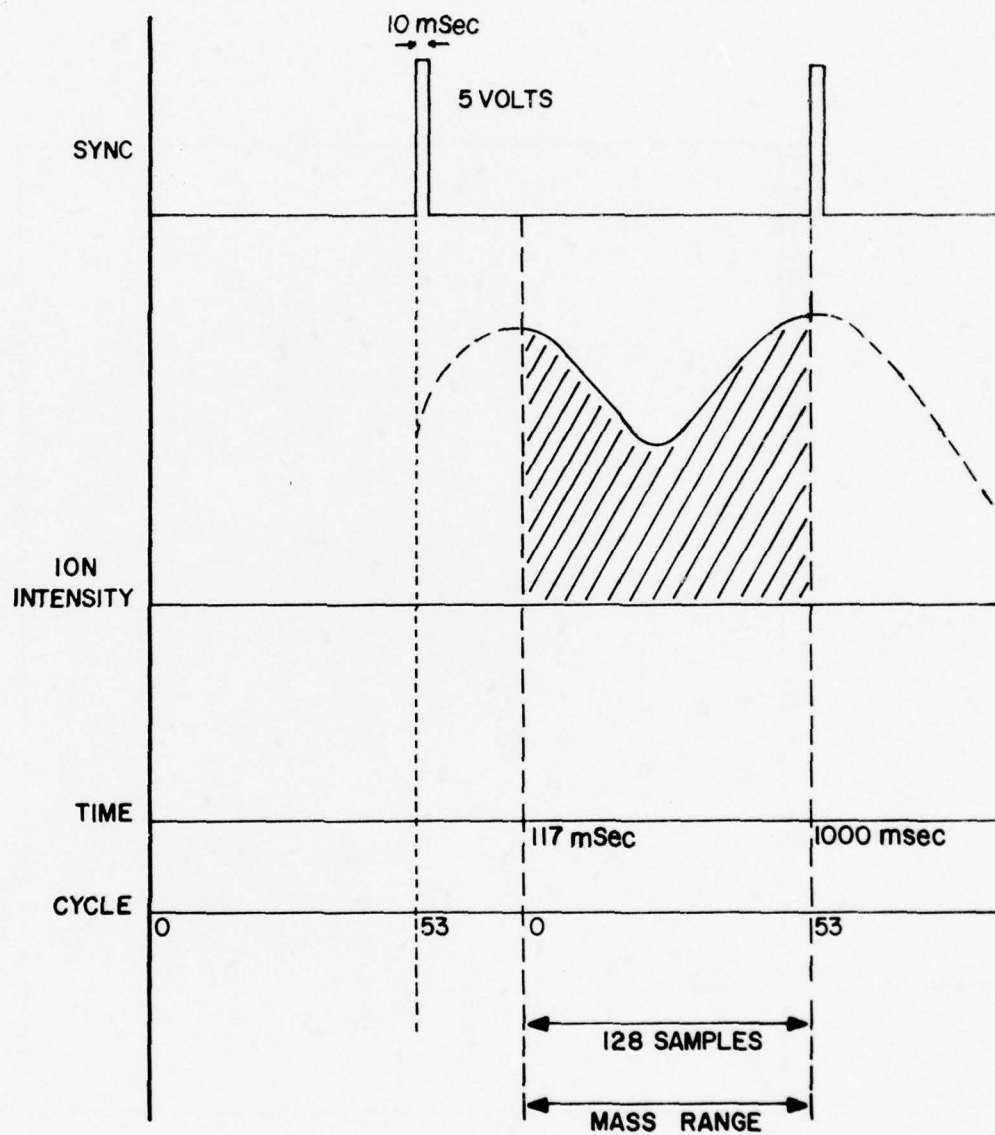


Fig. 9. Time Sequence of Events in the Data Acquisition Process

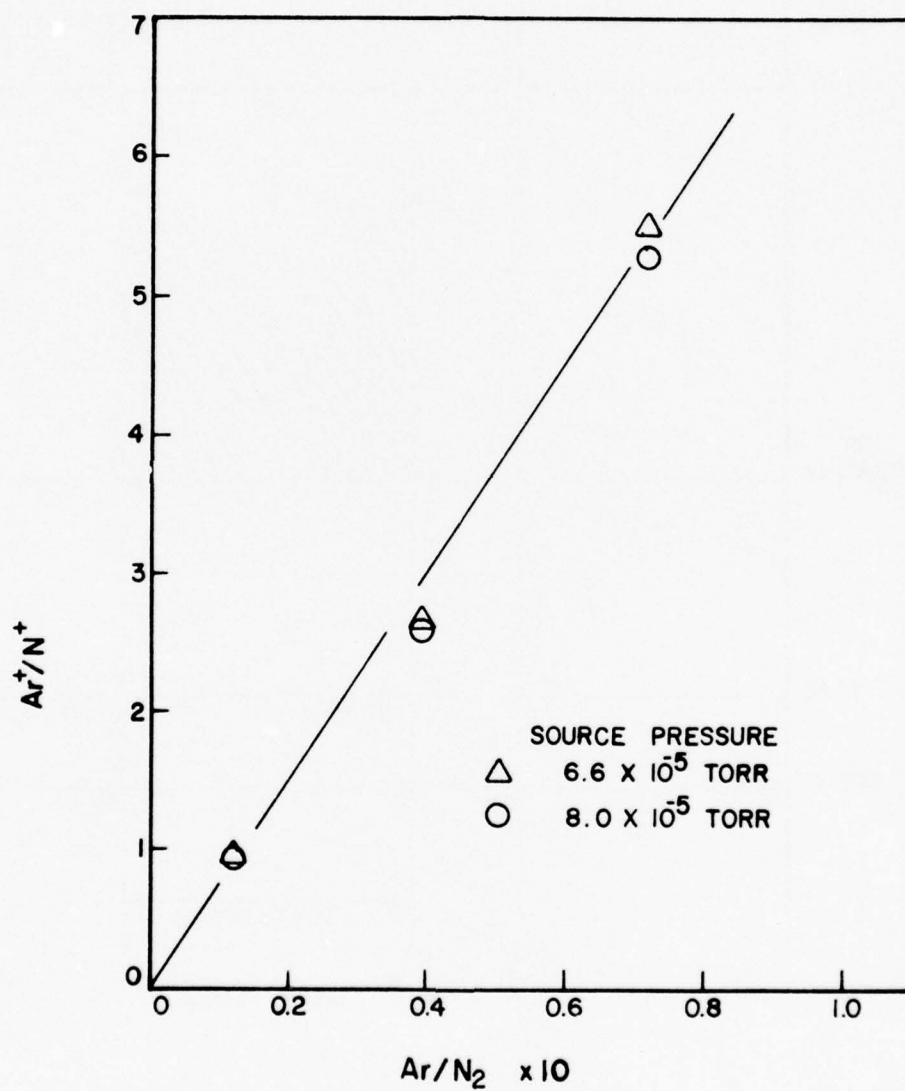


Fig. 10. Plot of Ion Intensity Ratio Ar^+/N^+ Versus the Argon/Nitrogen Mass Flow Ratio

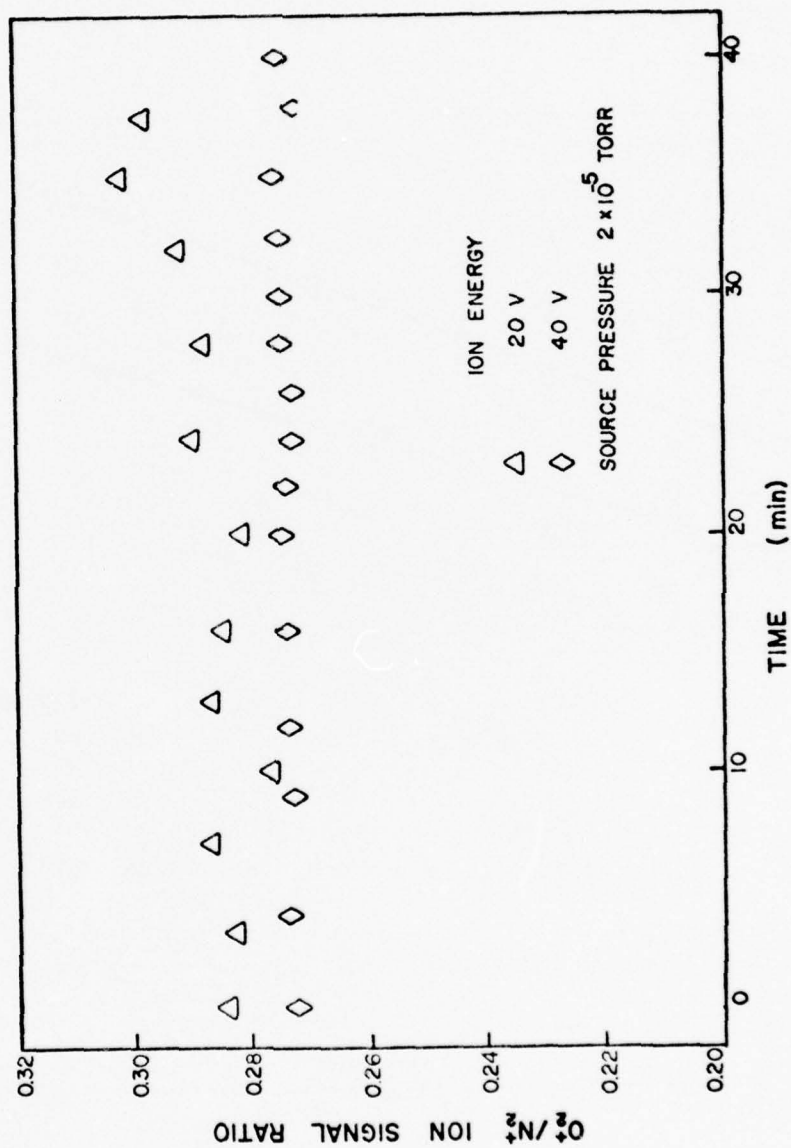


Fig. 11. Plots of Ion Intensity Ratio O_2^+/N_2^+ Versus Time

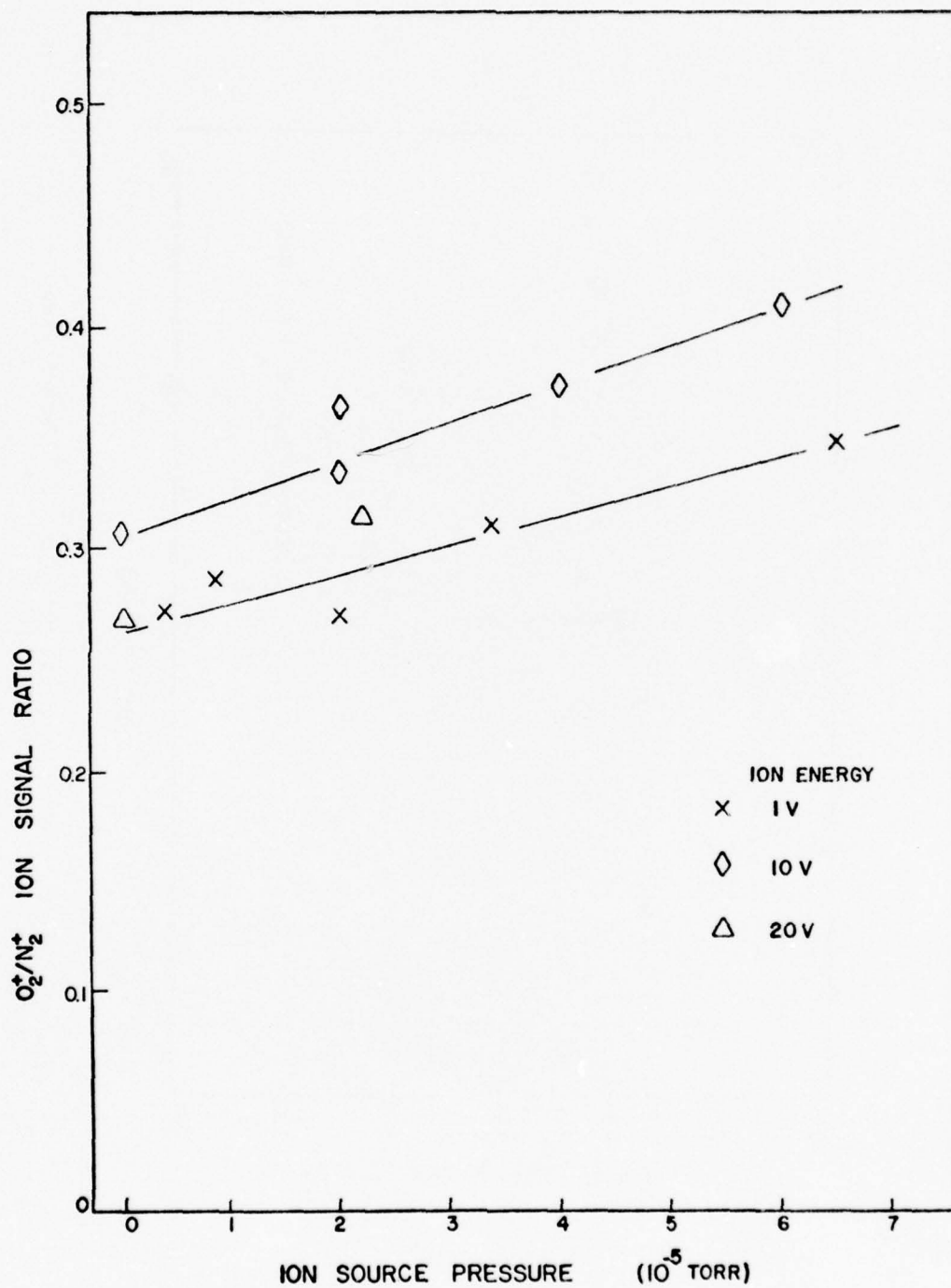


Fig. 12. Plots of Ion Intensity Ratio O_2^+/N_2^+ Versus Source Pressure for Ion Energies ≤ 20 Electron Volts

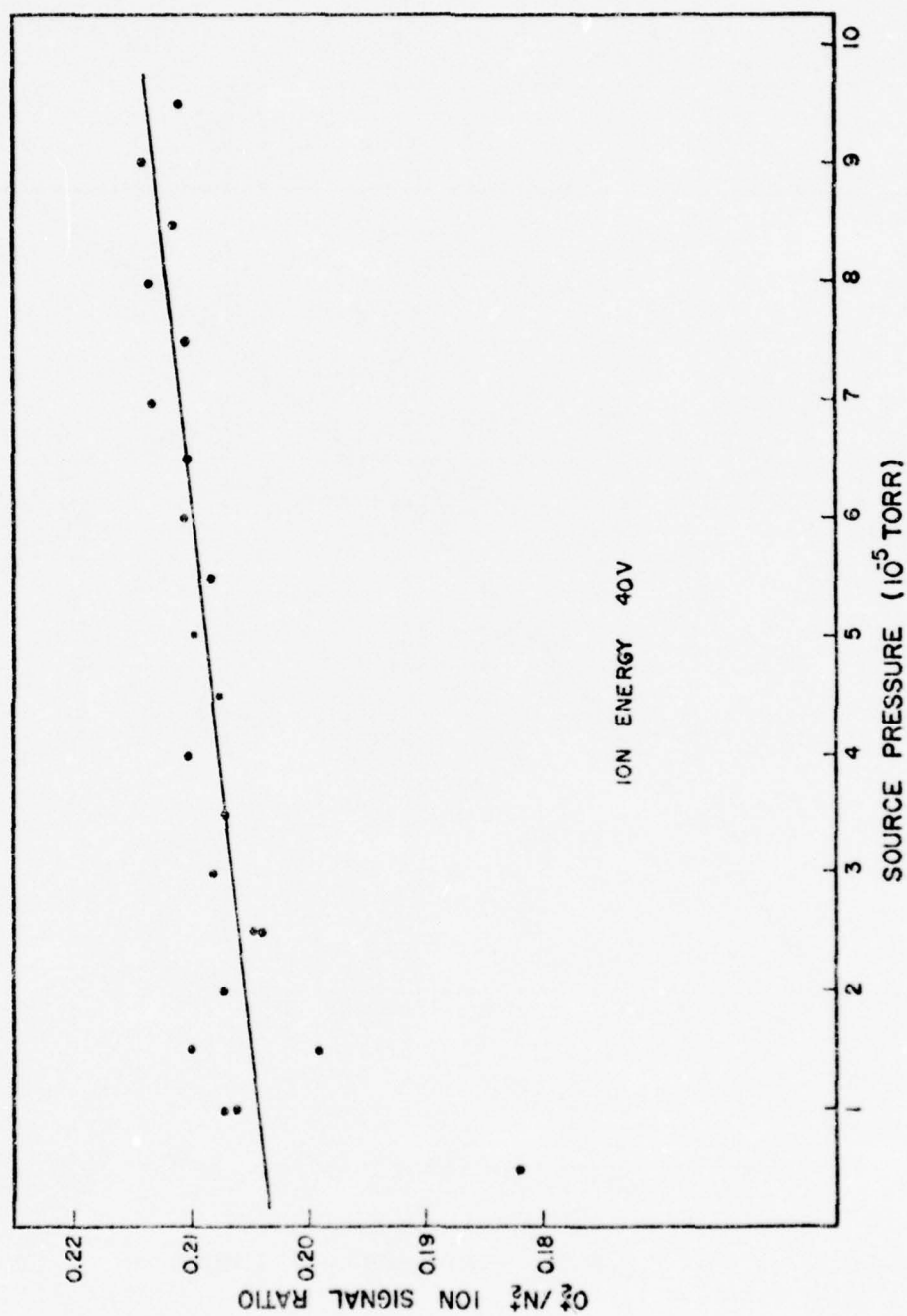


Fig. 13. Plot of Ion Intensity Ratio O_2^+/N_2^+ Versus Source Pressure for an Ion Energy of 40 Electron Volts

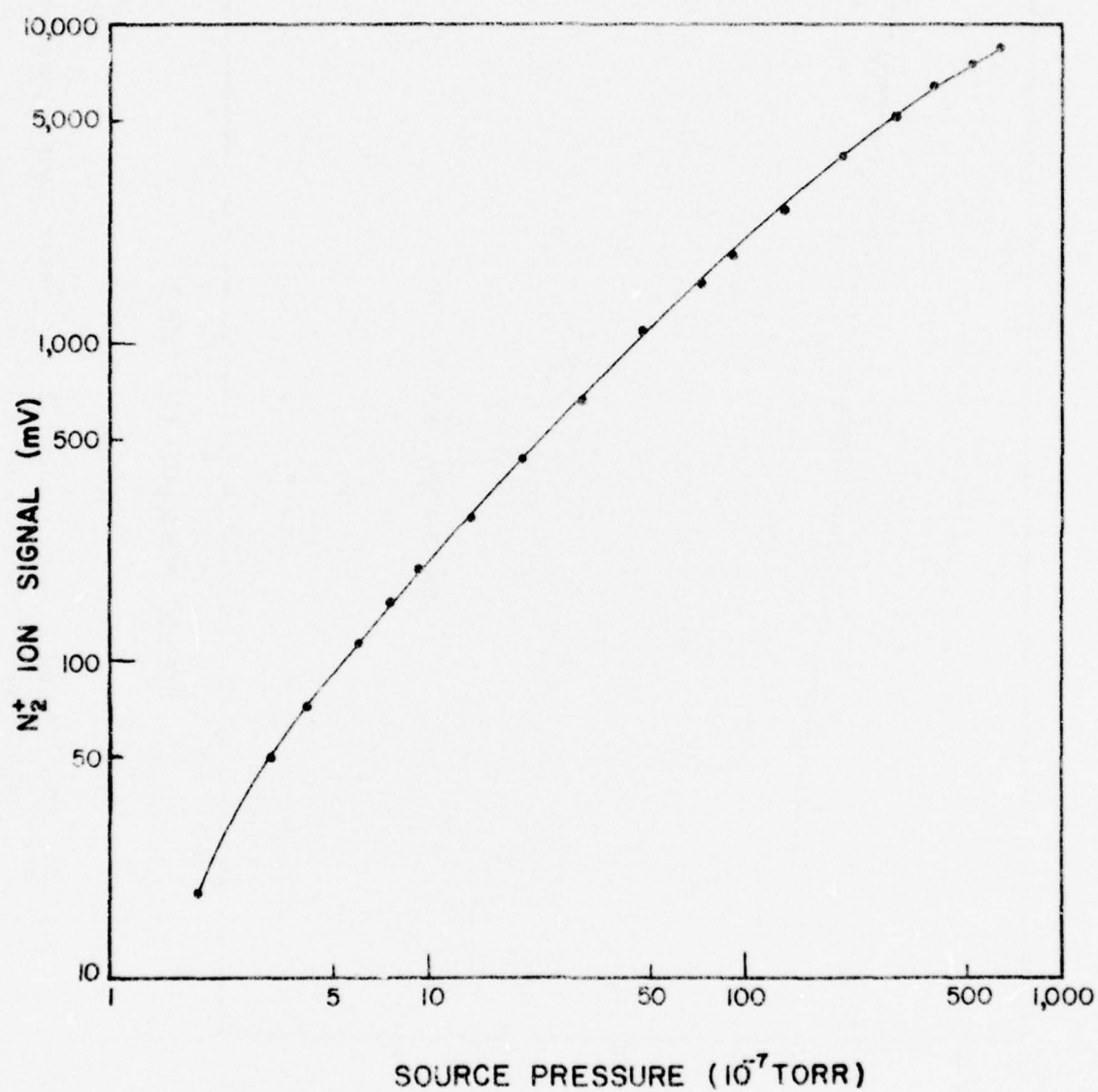


Fig. 14. Plot of N_2^+ Ion Signal Versus Source Pressure

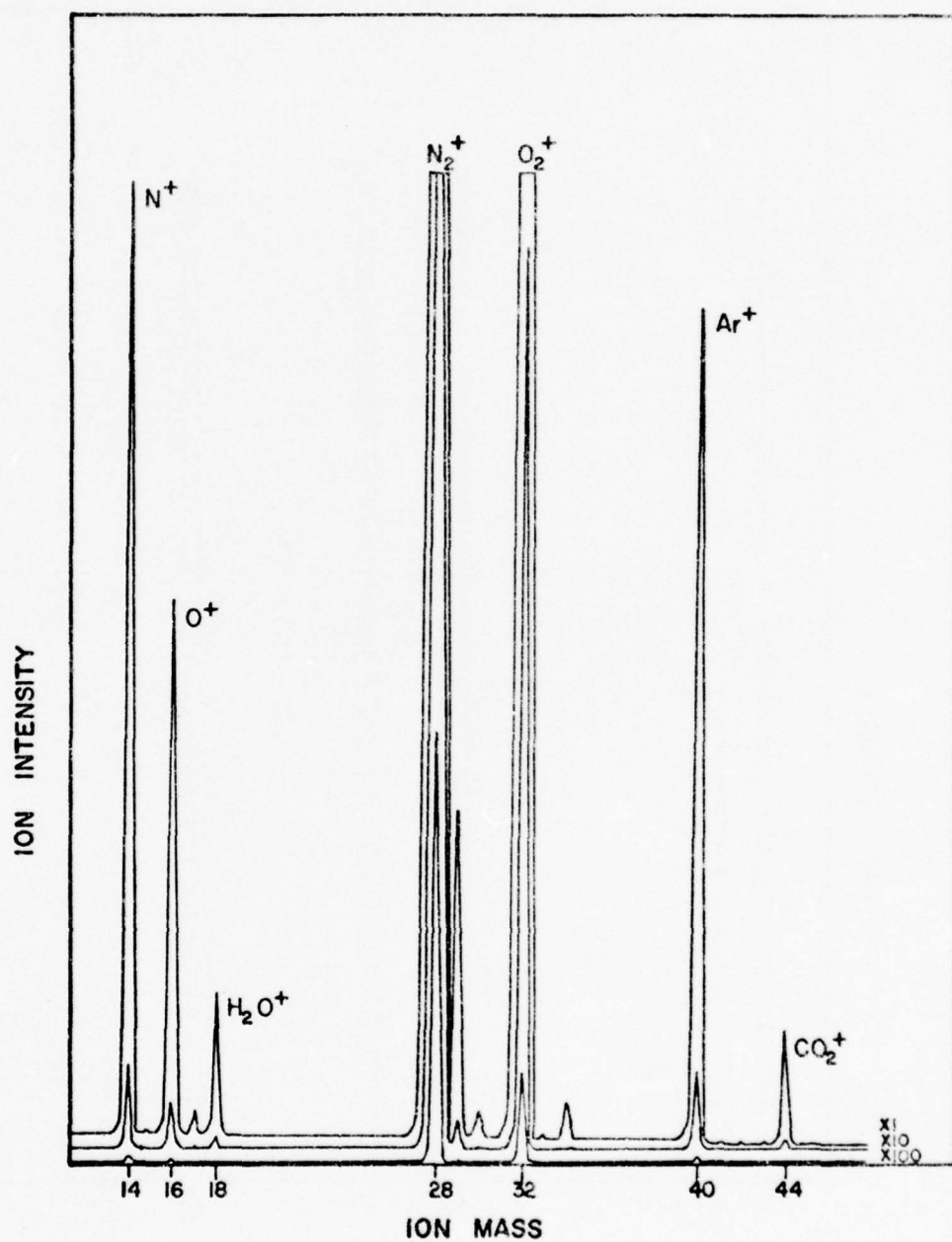


Fig. 15. Mass Spectrum of Ambient Air

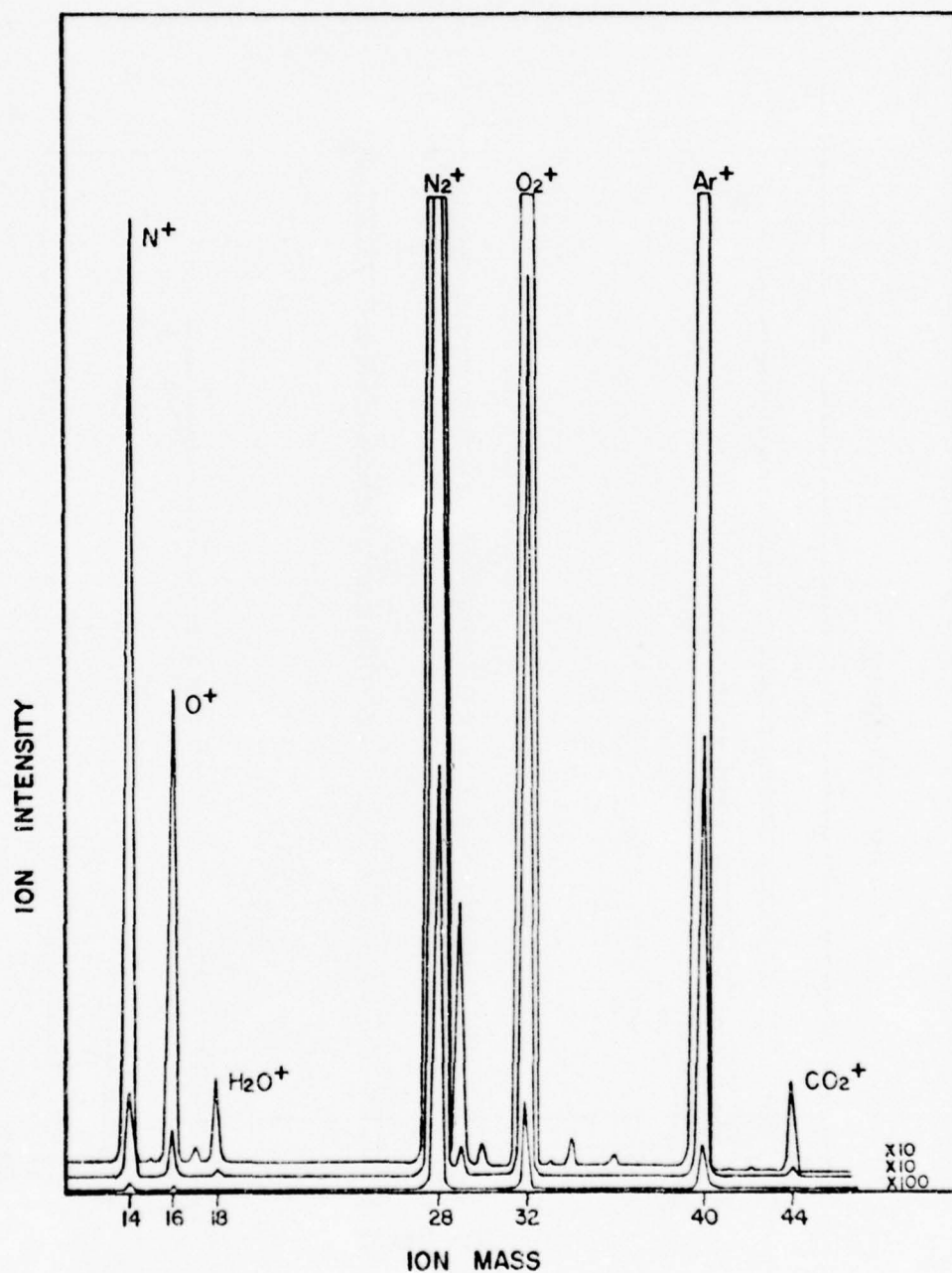


Fig. 16. Mass Spectrum of Compressed Air/Injected Argon

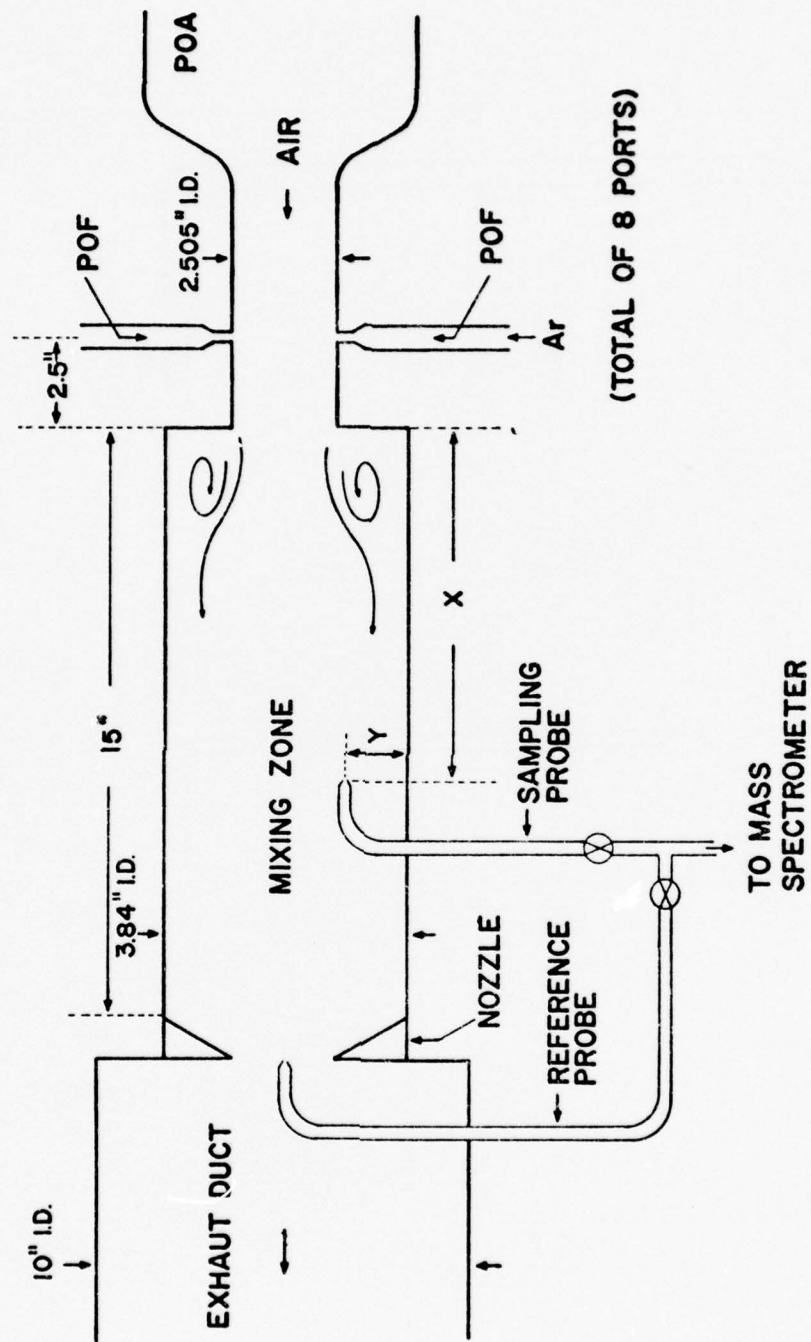
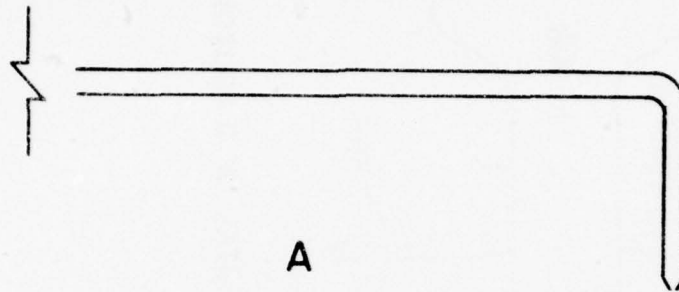
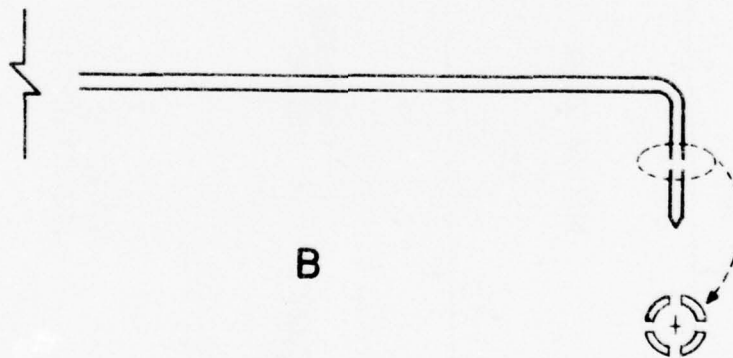


Fig. 17. Schematic Diagram of the Combustor and Gas Sampling System



A



B

Fig. 18. Schematic Diagram of the Sampling Probes (A. Impact Probe. B. Static Probe.)

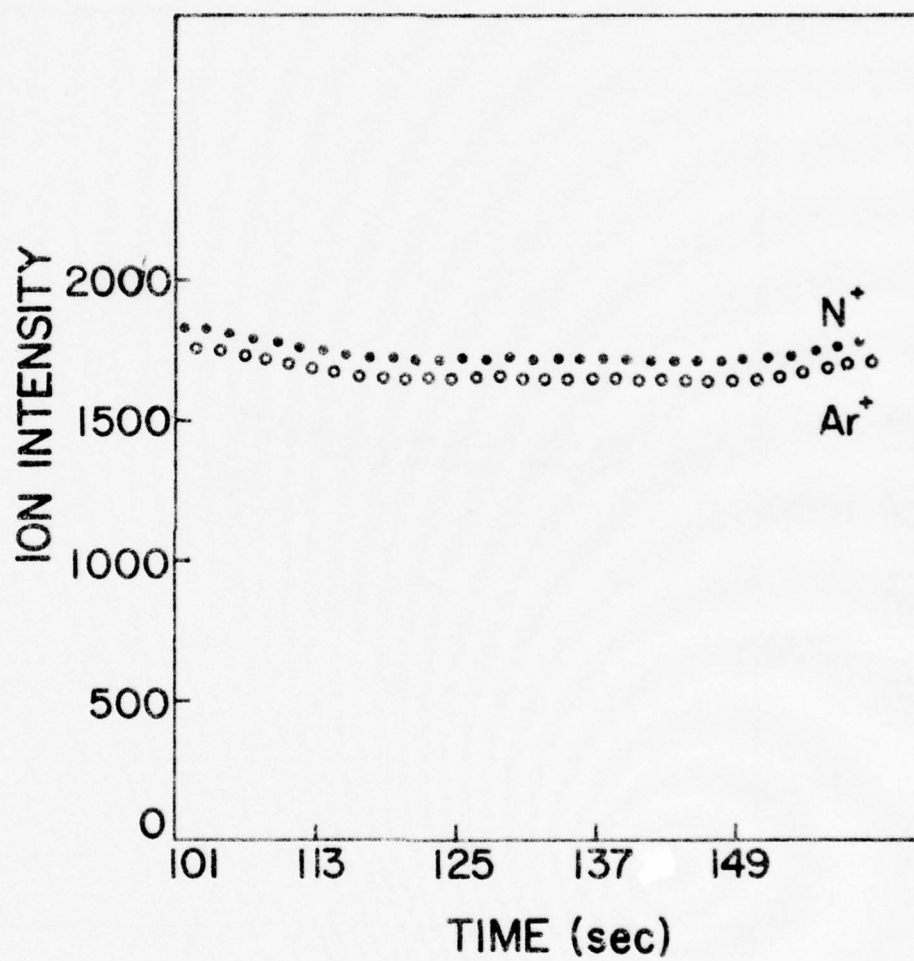


Fig. 19a. Time Profiles of the N^+ and Ar^+ Signals During a Typical Combustor Experiment (No Injected Argon)

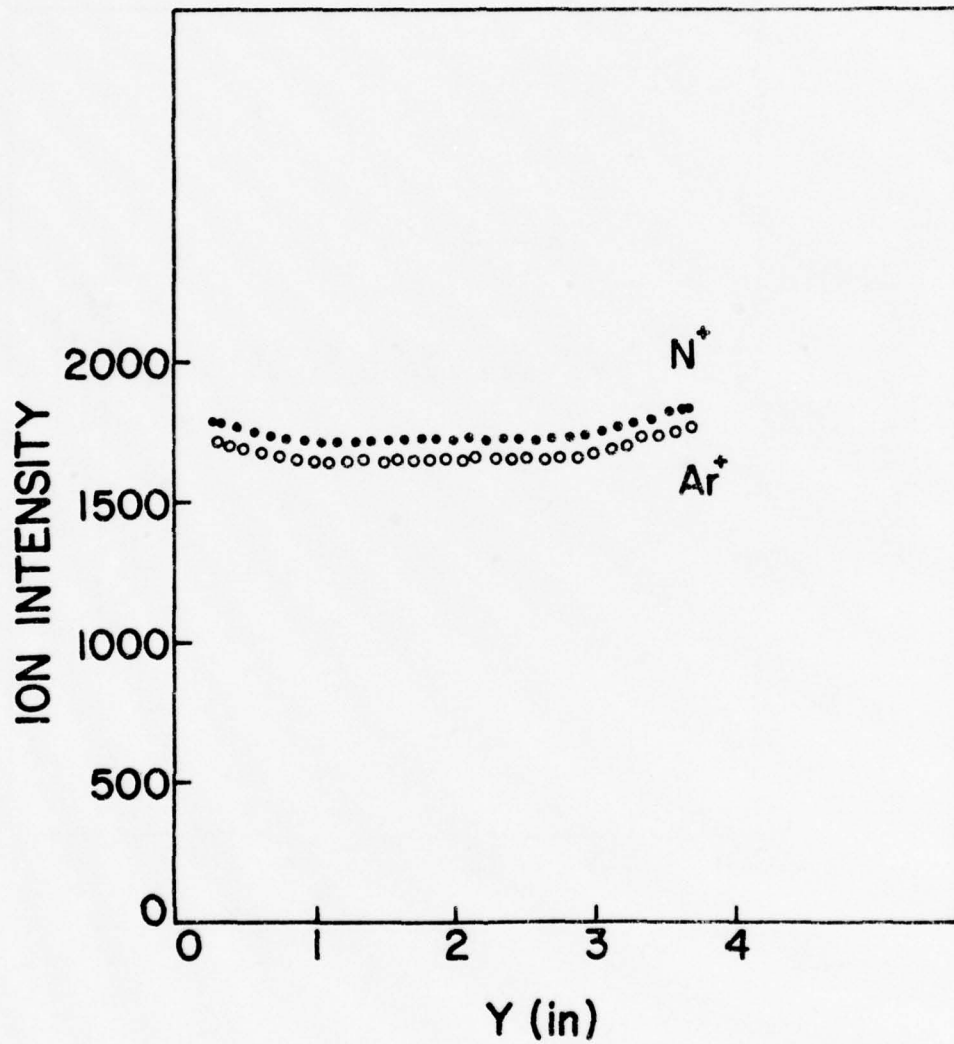


Fig. 19b. Radial Profiles of the N^+ and Ar^+ Signals During a Typical Combustor Experiment (No Injected Argon)

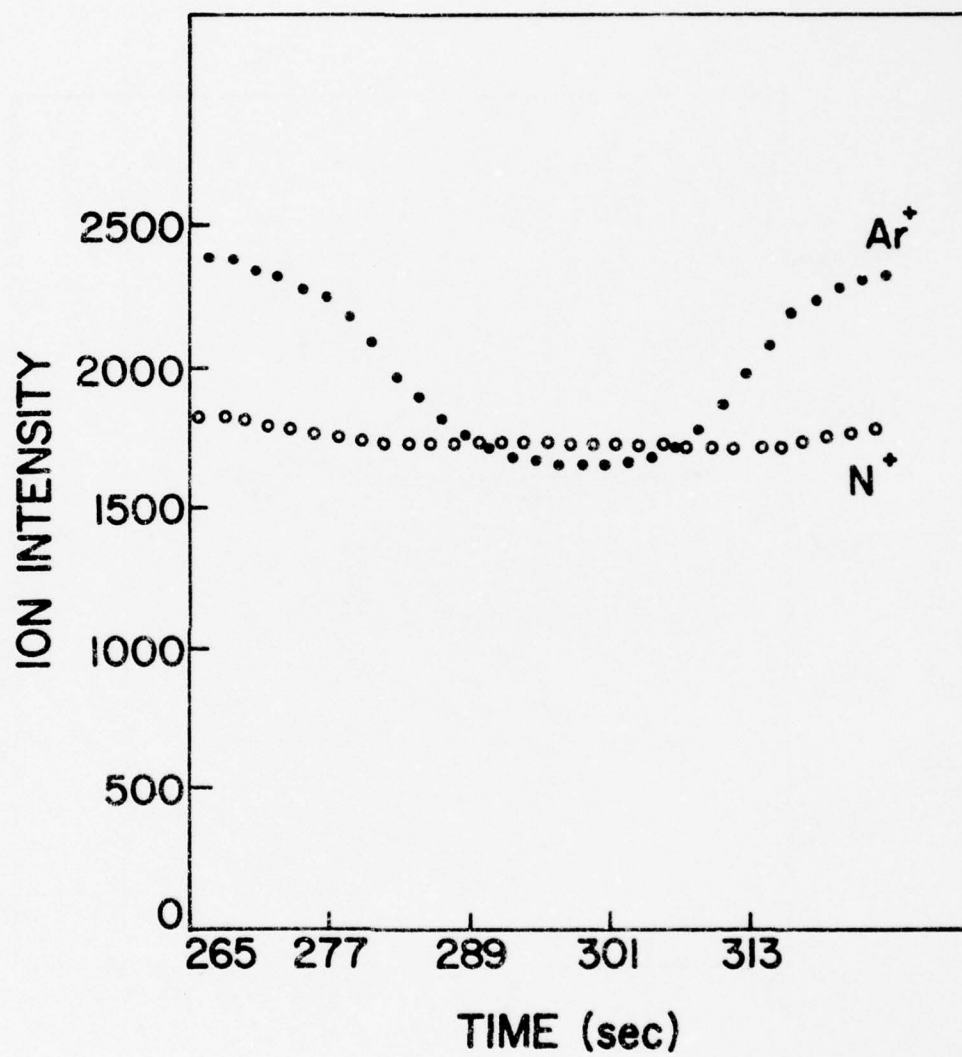


Fig. 20a. Time Profiles of the N^+ and Ar^+ Signals During a Typical Combustor Experiment (With Injected Argon)

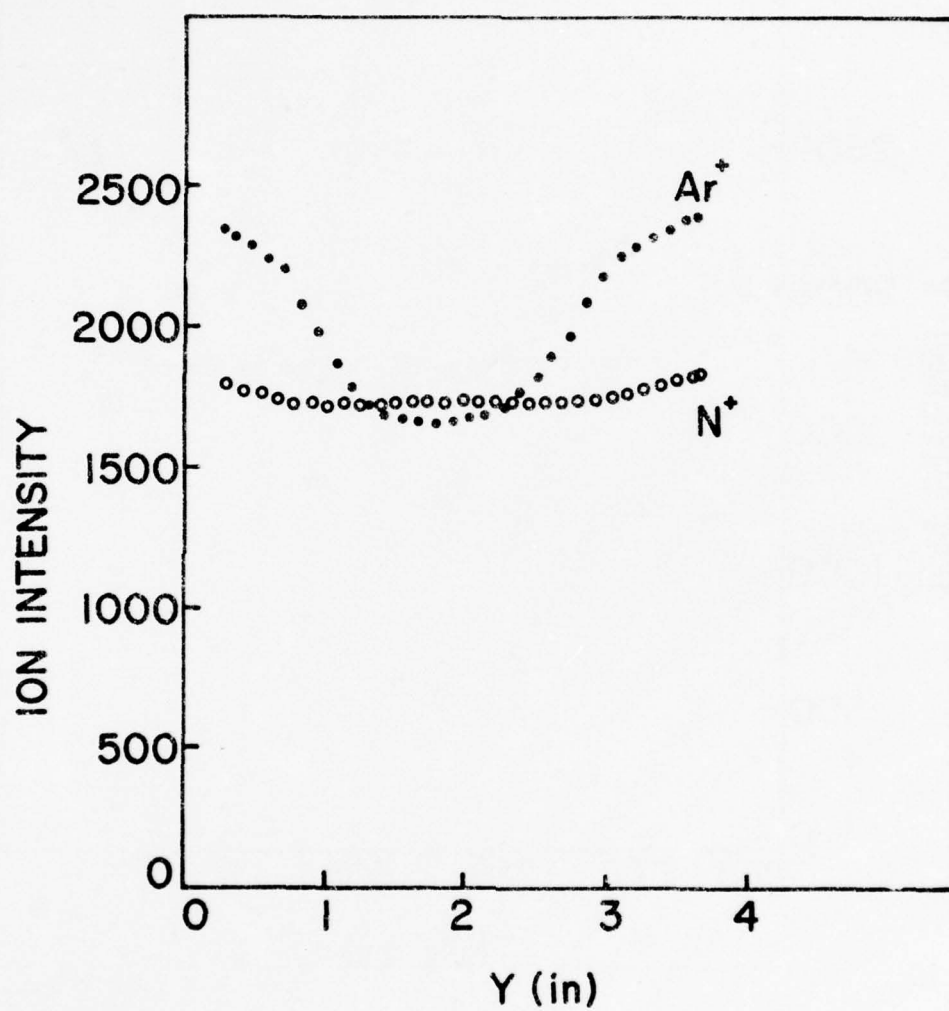


Fig. 20b. Radial Profiles of the N^+ and Ar^+ Signals During a Typical Combustor Experiment (With Injected Argon)

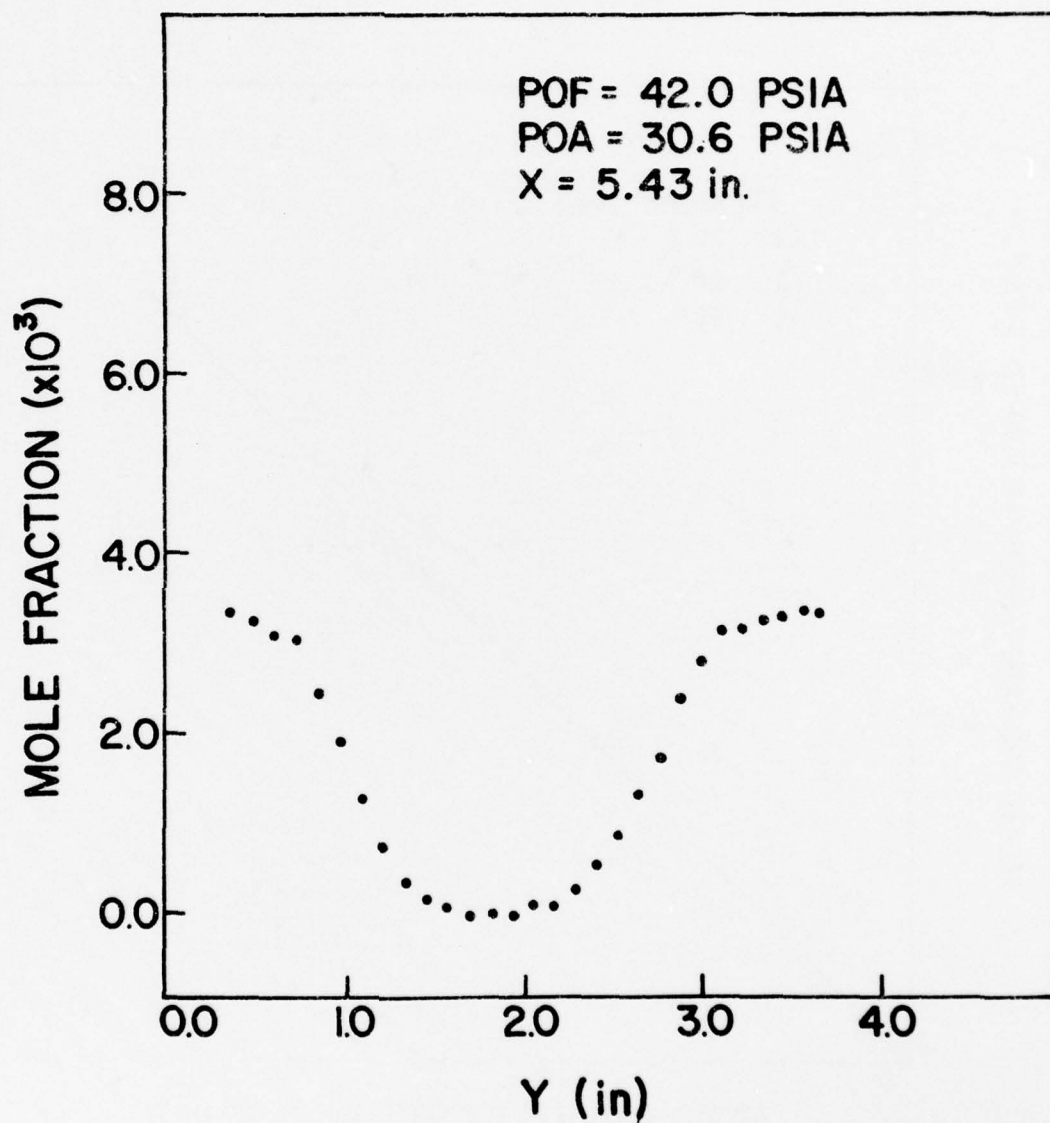


Fig. 21. Mole Fraction of Injected Argon Versus the Radial Position of the Sampling Probe

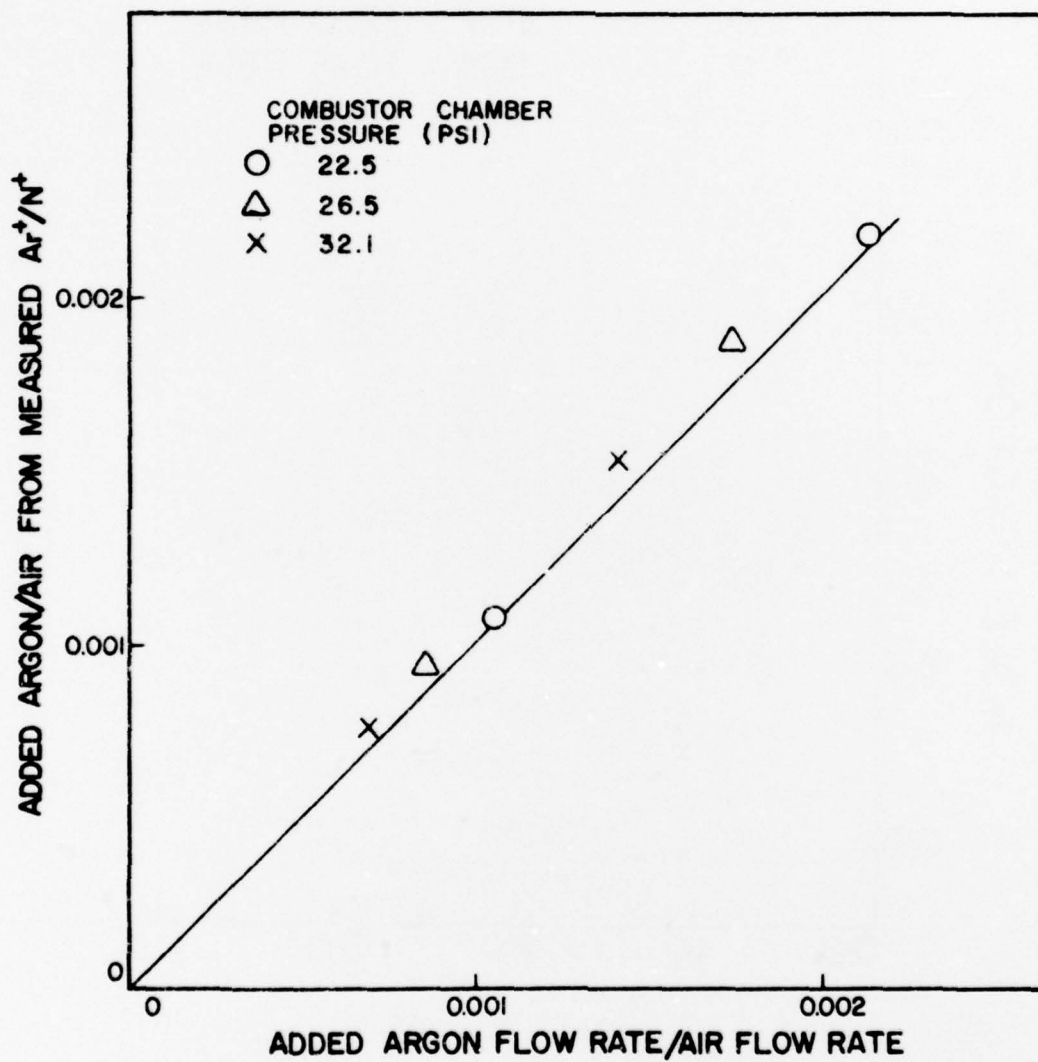


Fig. 22. Comparison of the Injected Argon/Air Ratios Calculated from Measured Ar^+/N^+ Ratios with Those Calculated from the Measured Argon and Air Mass Flow Rates

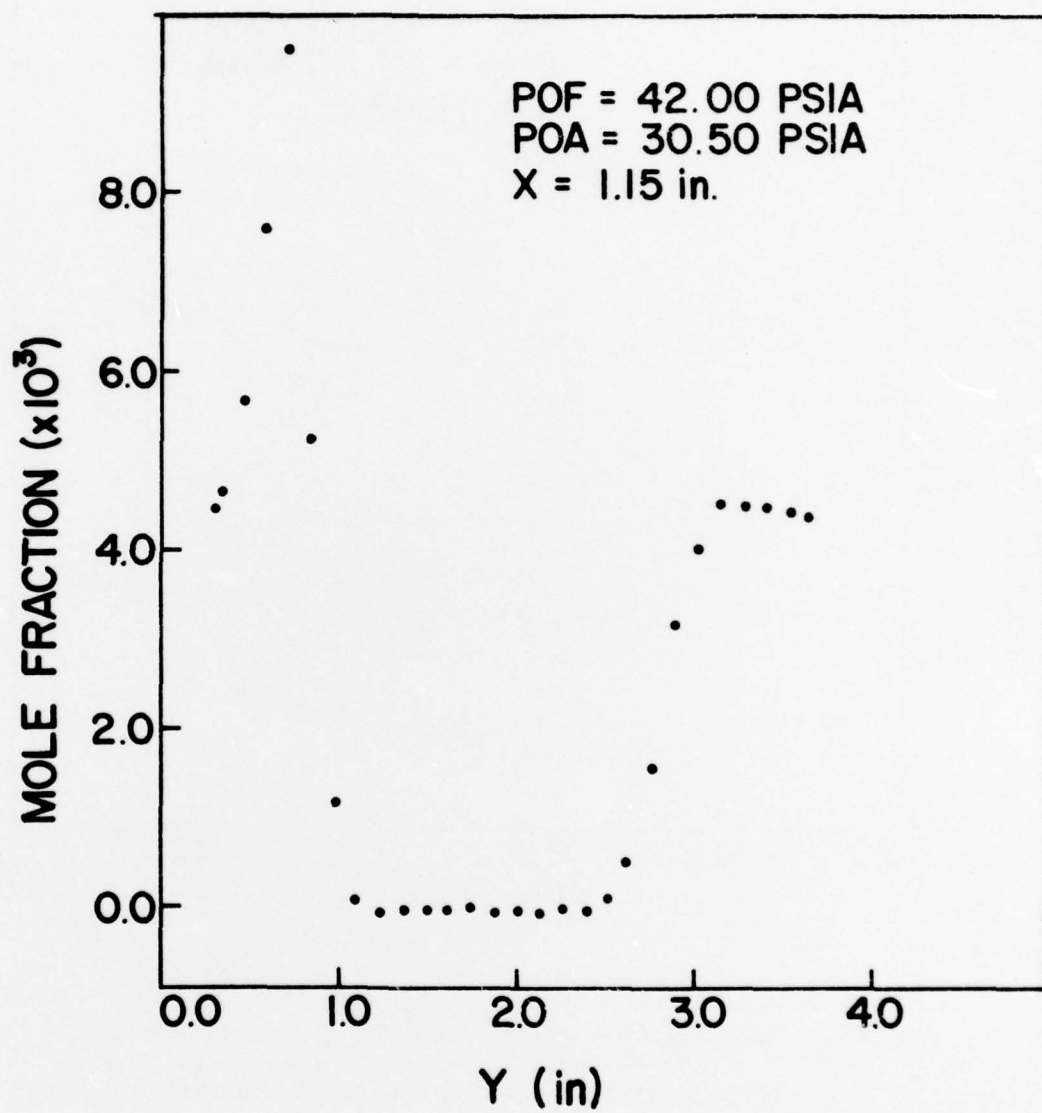


Fig. 23a. Mole Fraction of Injected Argon Versus the Radial Position of the Sampling Probe (see Table II for experimental conditions applicable to this figure)

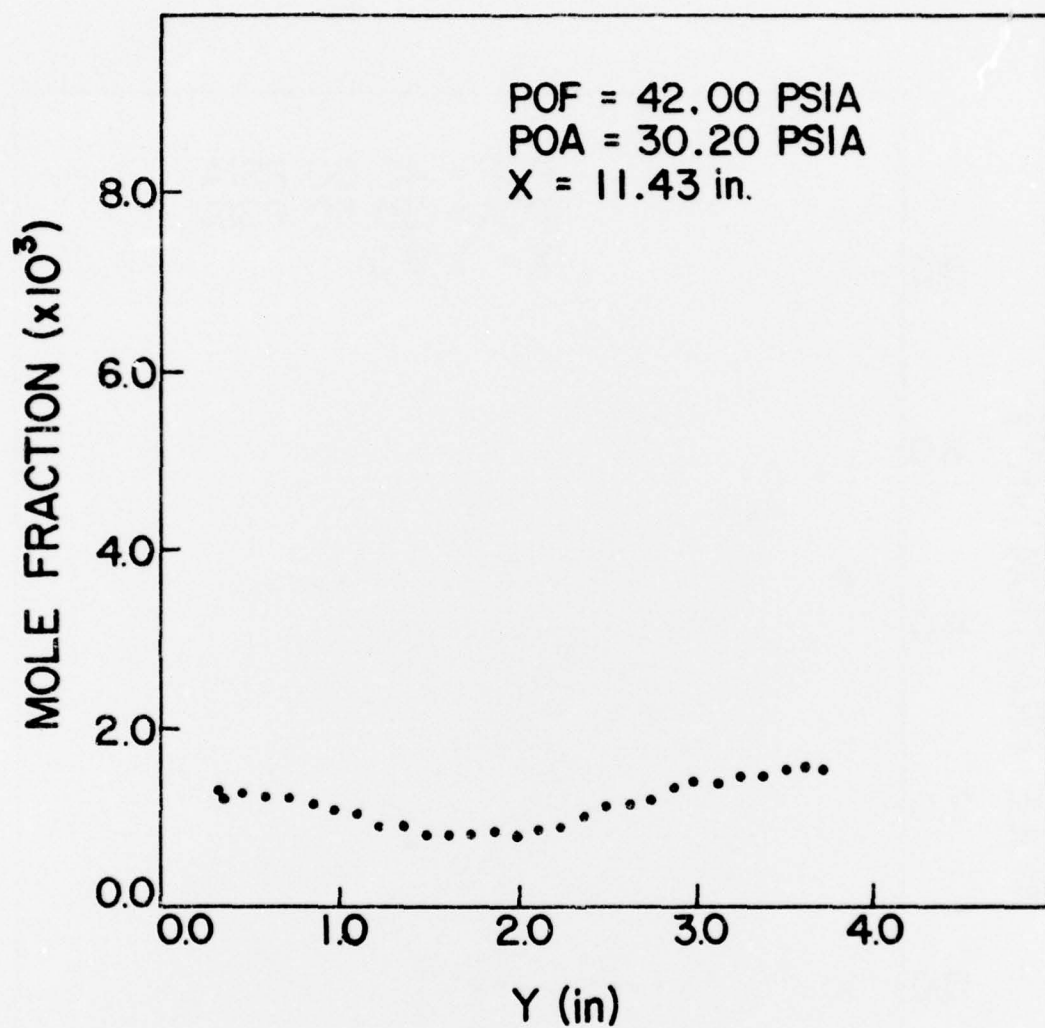


Fig. 23b. Mole Fraction of Injected Argon Versus the Radial Position of the Sampling Probe (see Table II for experimental conditions applicable to this figure)

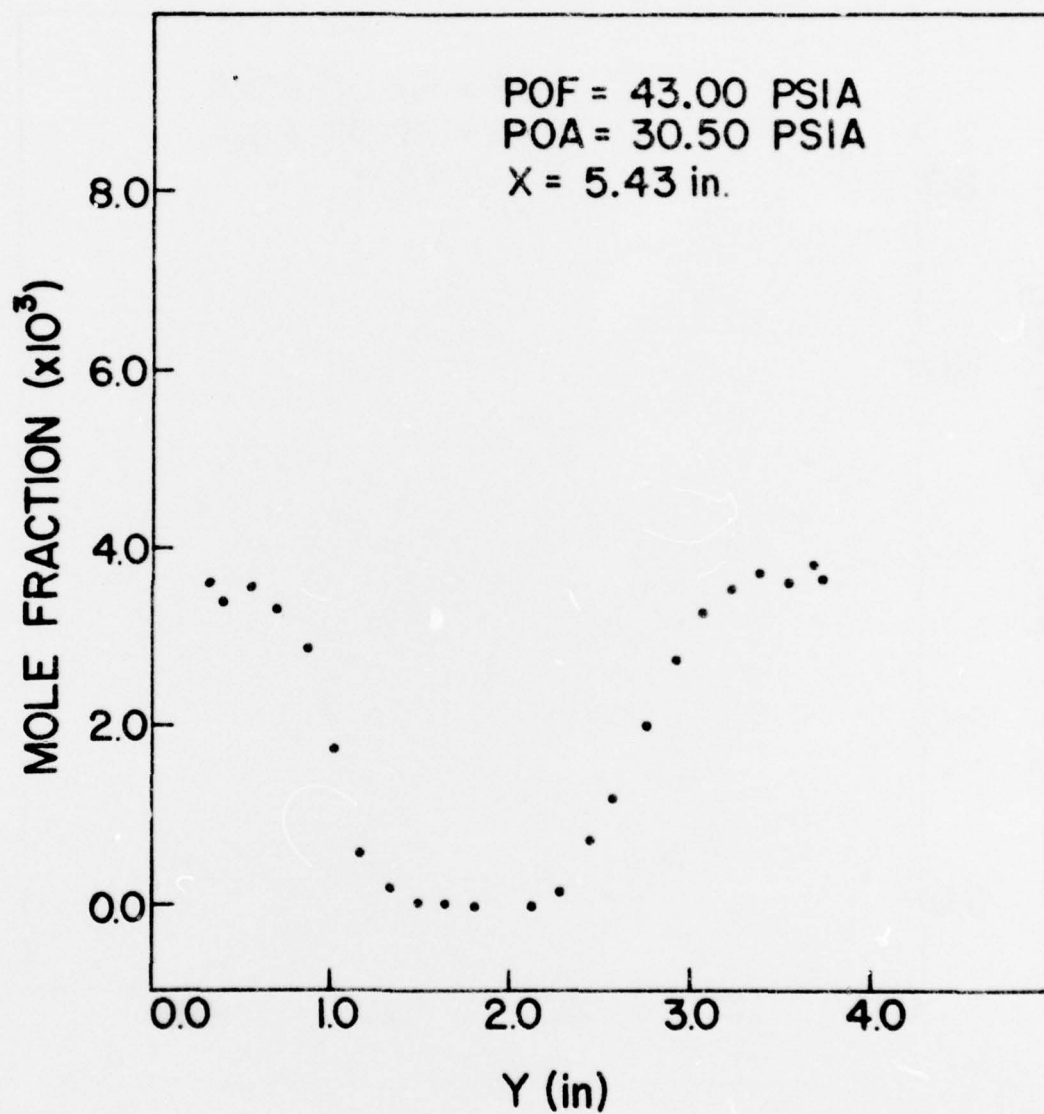


Fig. 23c. Mole Fraction of Injected Argon Versus the Radial Position of the Sampling Probe (see Table II for experimental conditions applicable to this figure)

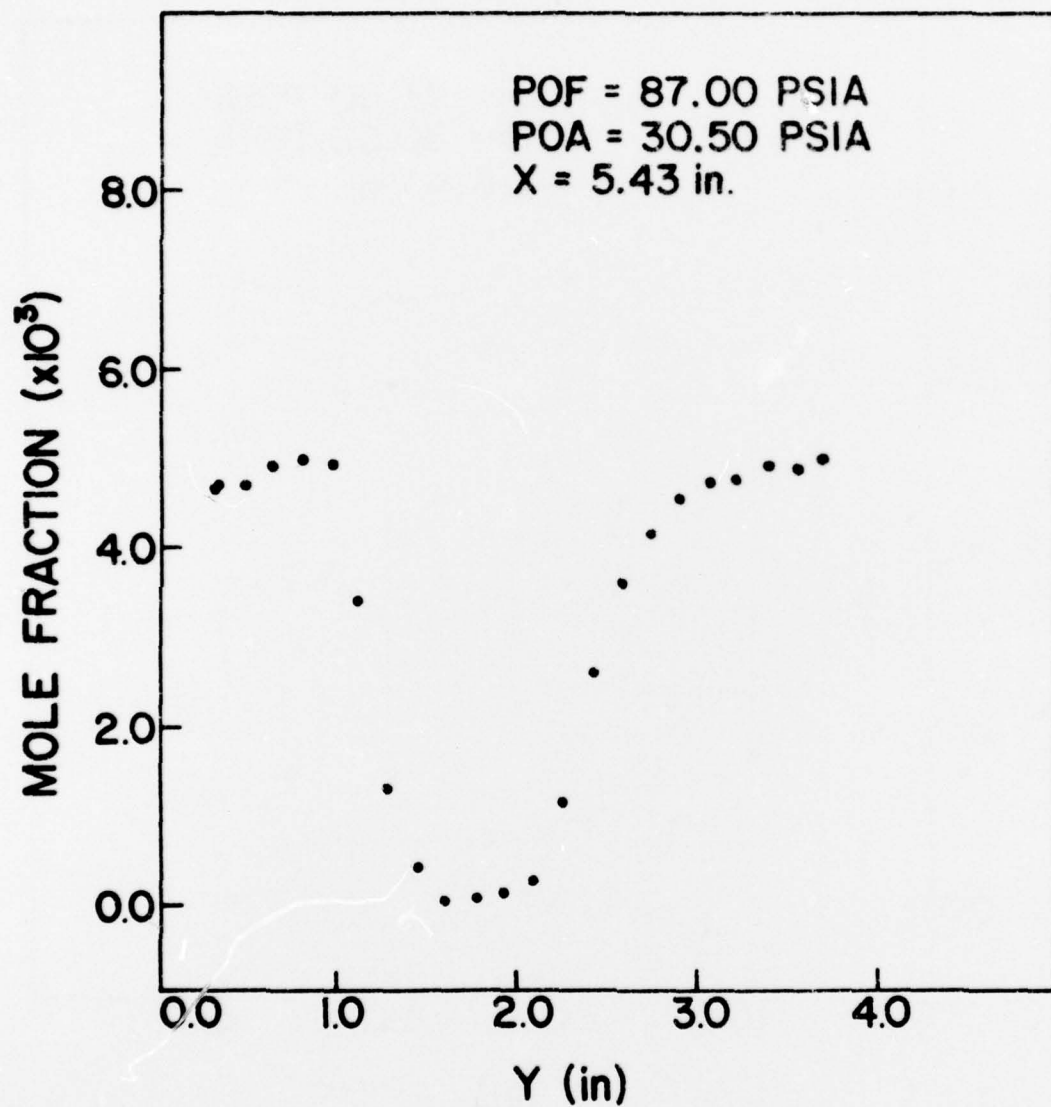


Fig. 23d. Mole Fraction of Injected Argon Versus the Radial Position of the Sampling Probe (see Table II for experimental conditions applicable to this figure)

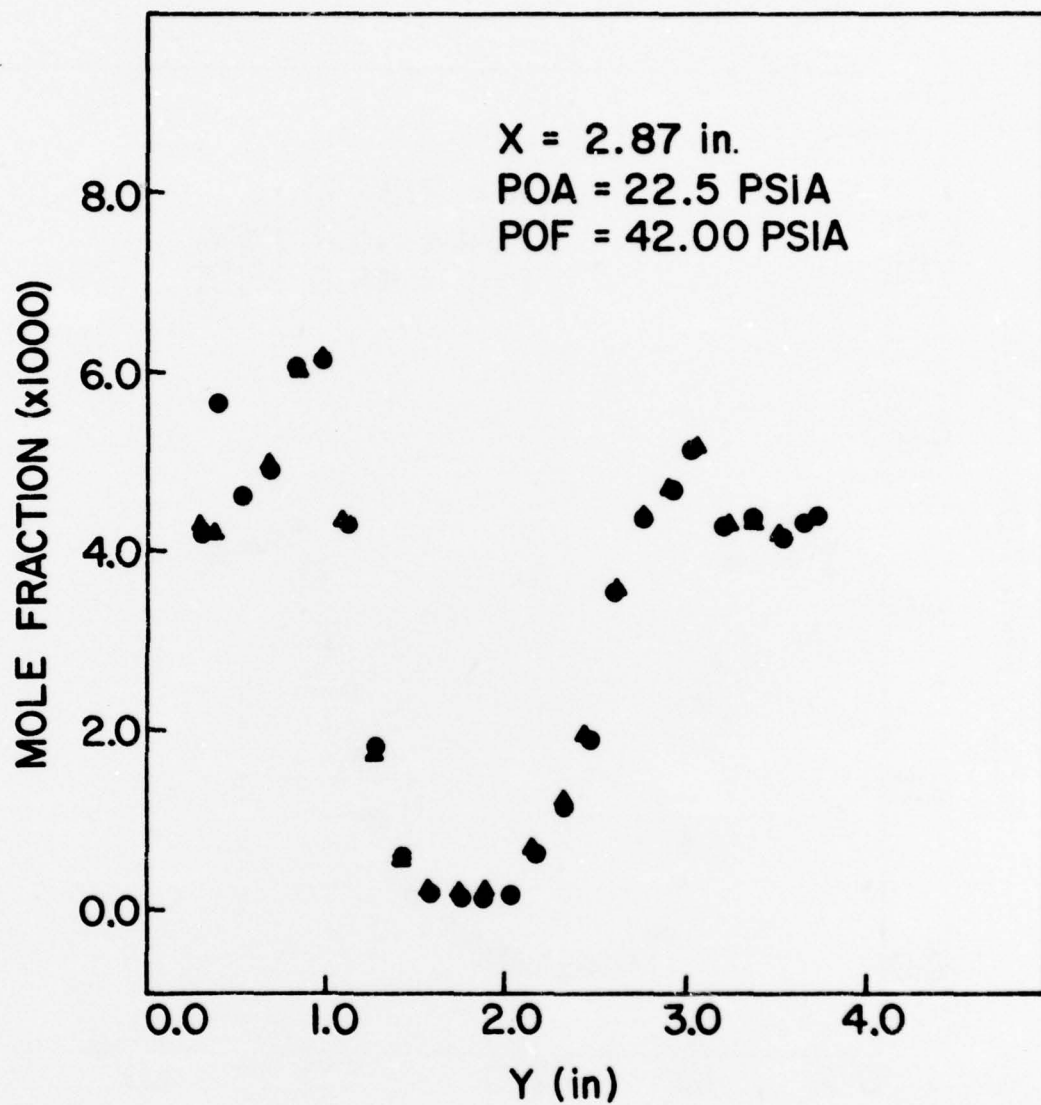


Fig. 23e. Mole Fraction of Injected Argon Versus the Radial Position of the Sampling Probe (see Table II for experimental conditions applicable to this figure)

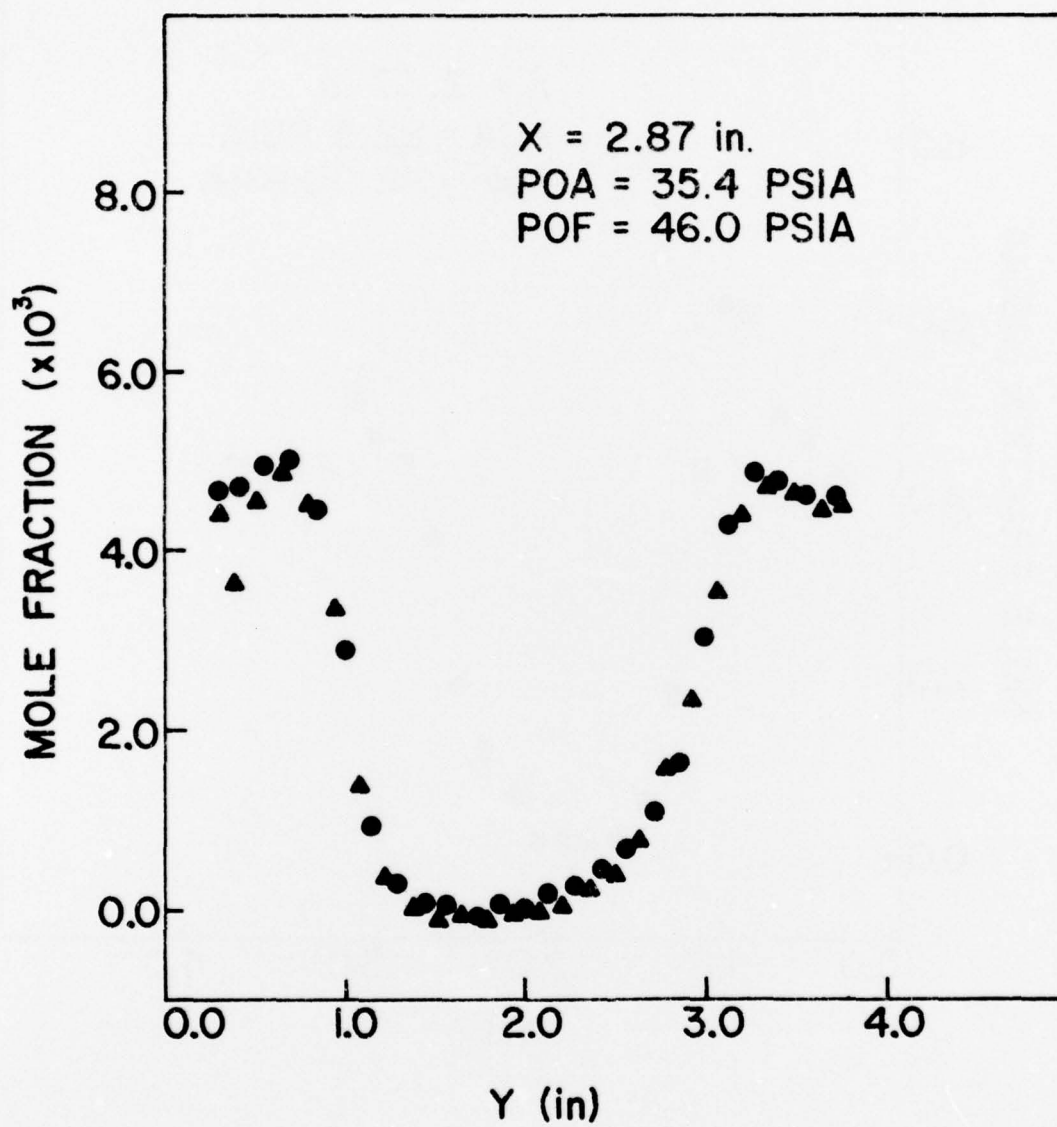


Fig. 23f. Mole Fraction of Injected Argon Versus the Radial Position of the Sampling Probe (see Table II for experimental conditions applicable to this figure)

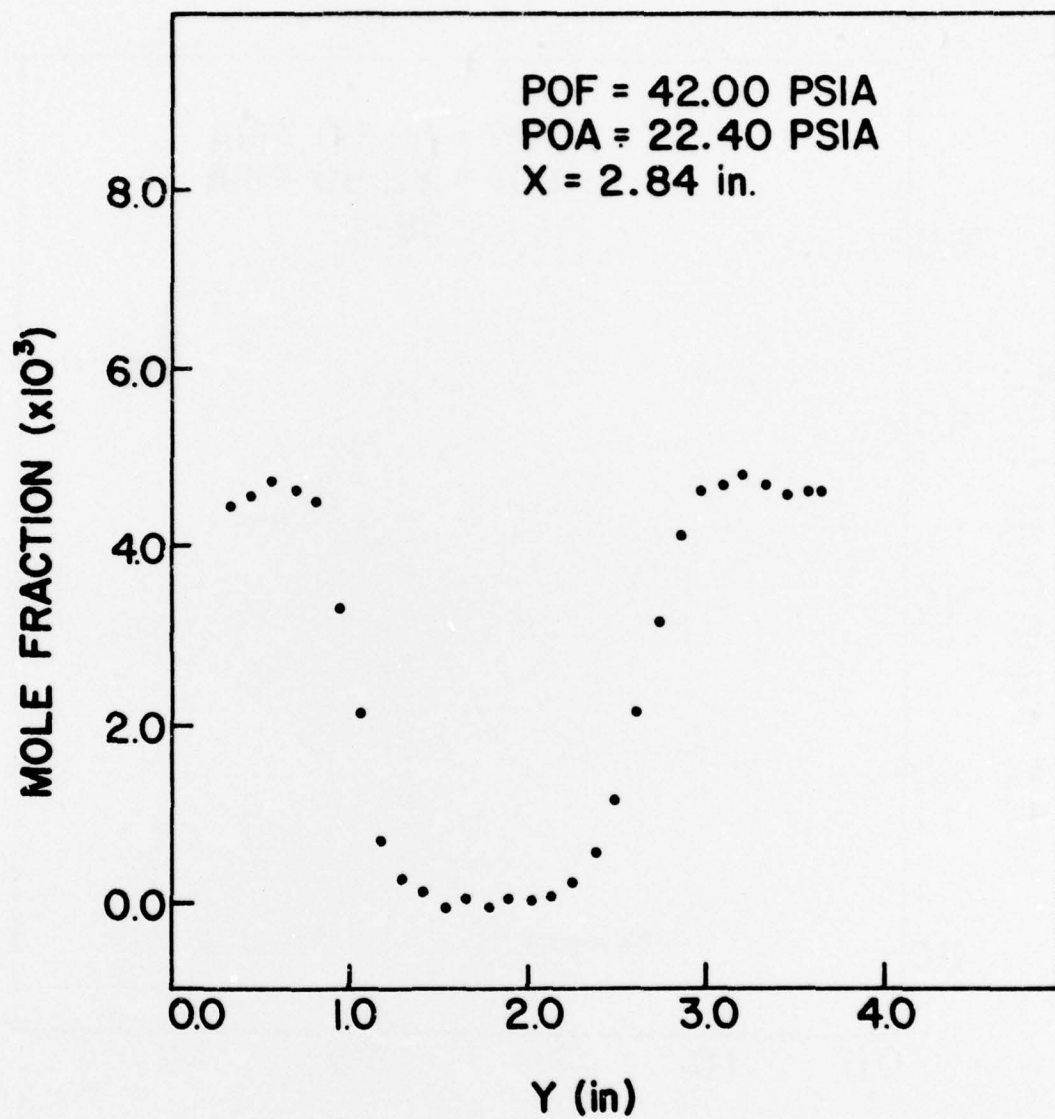


Fig. 23g. Mole Fraction of Injected Argon Versus the Radial Position of the Sampling Probe (see Table II for experimental conditions applicable to this figure)

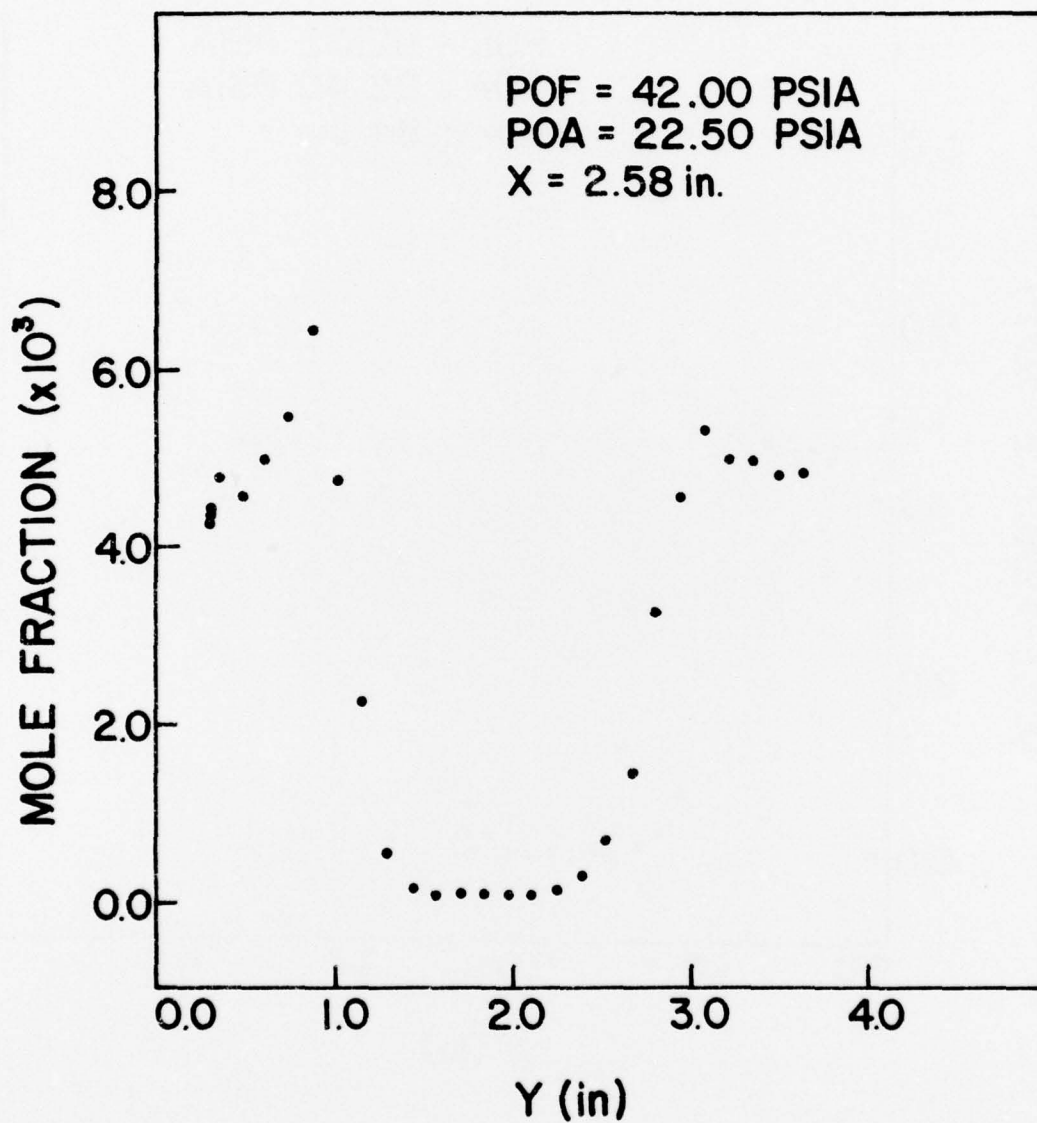


Fig. 23h. Mole Fraction of Injected Argon Versus the Radial Position of the Sampling Probe (see Table II for experimental conditions applicable to this figure)

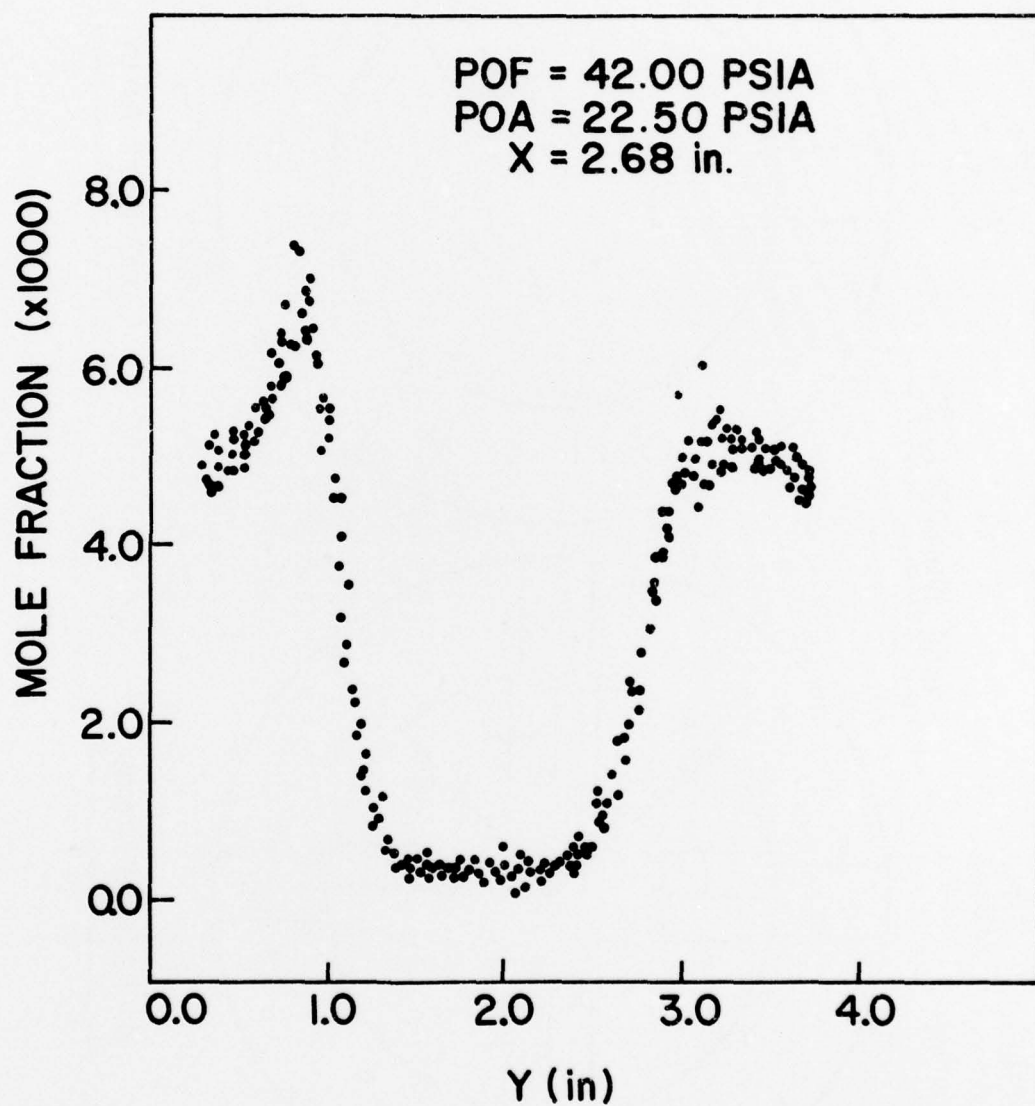
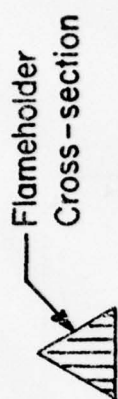
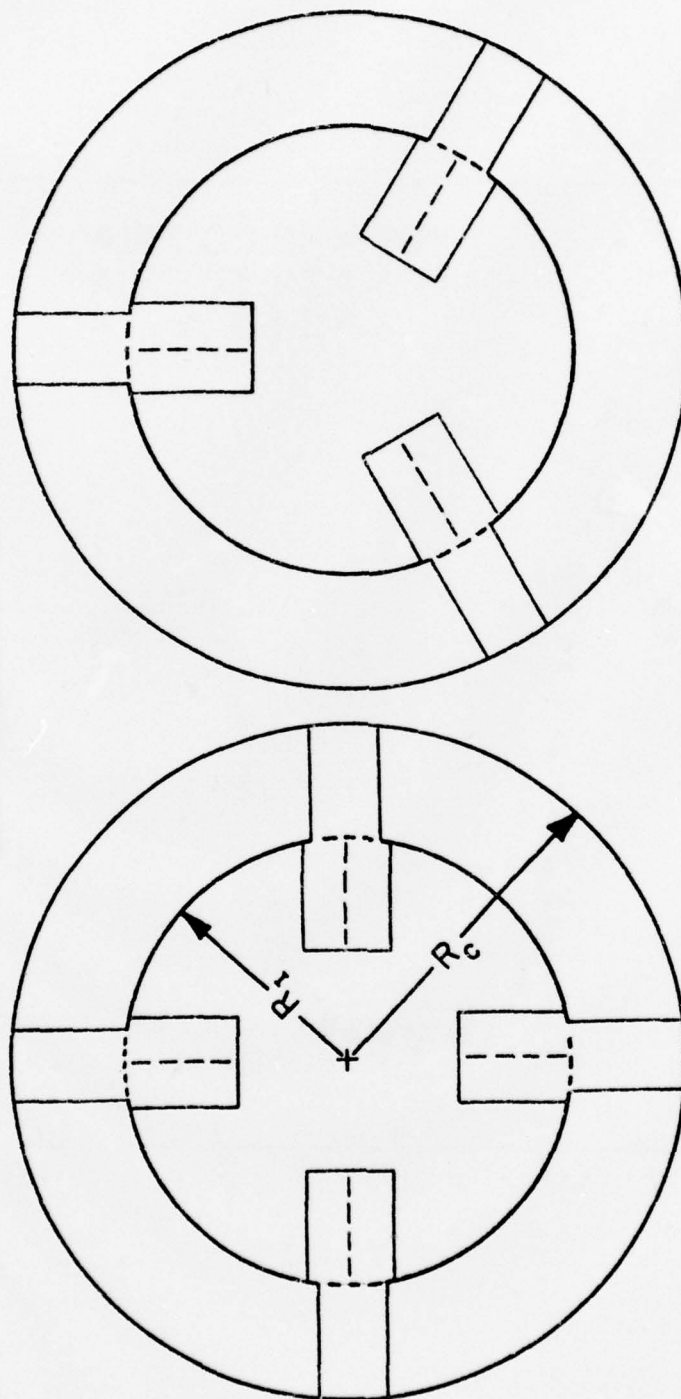


Fig. 23i. Mole Fraction of Injected Argon Versus the Radial Position of the Sampling Probe (see Table II for experimental conditions applicable to this figure)



Inlet Blockage : 25%



3 - Element Array

4 - Element Array

Fig. 24. Schematic Diagram of the Flame Holders (4-element array and 3-element array)

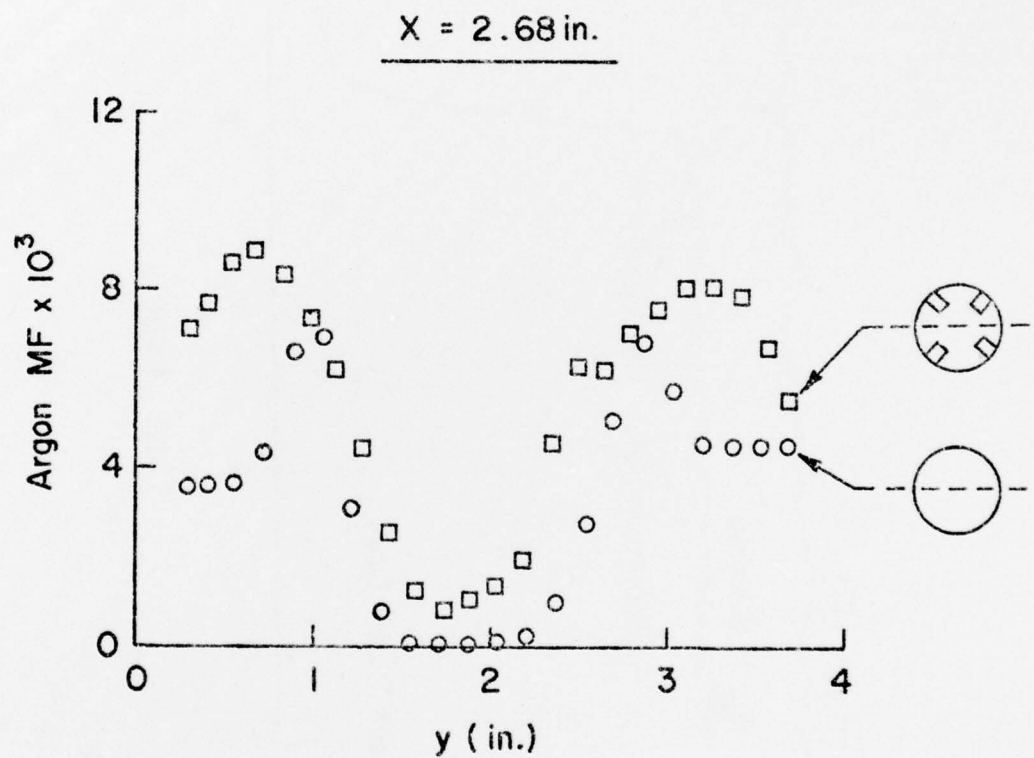


Fig. 25. Comparison of the Injected Argon Concentration Profiles Obtained With and Without the Flame Holder

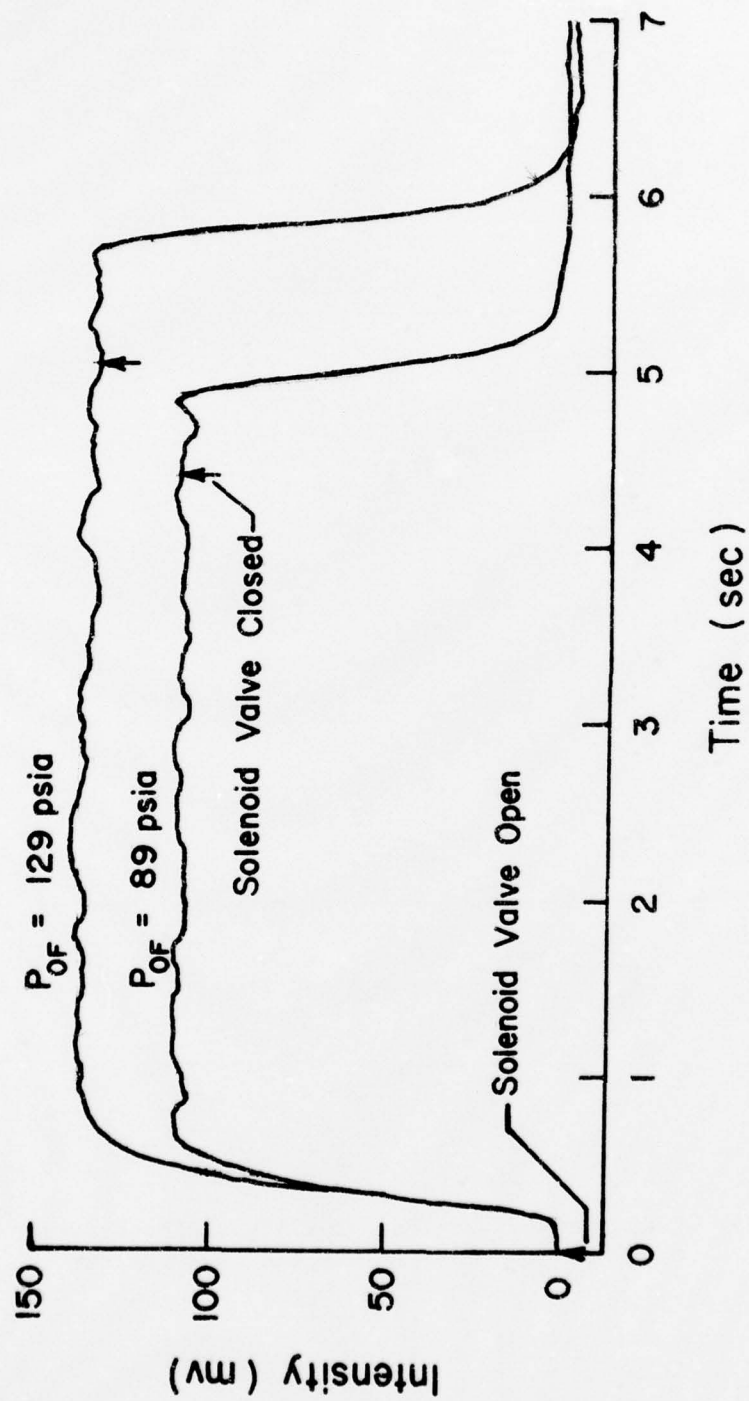


Fig. 26. Plots of Argon Ion Signal Time Response for Gas Sampled from the Sampling Probe

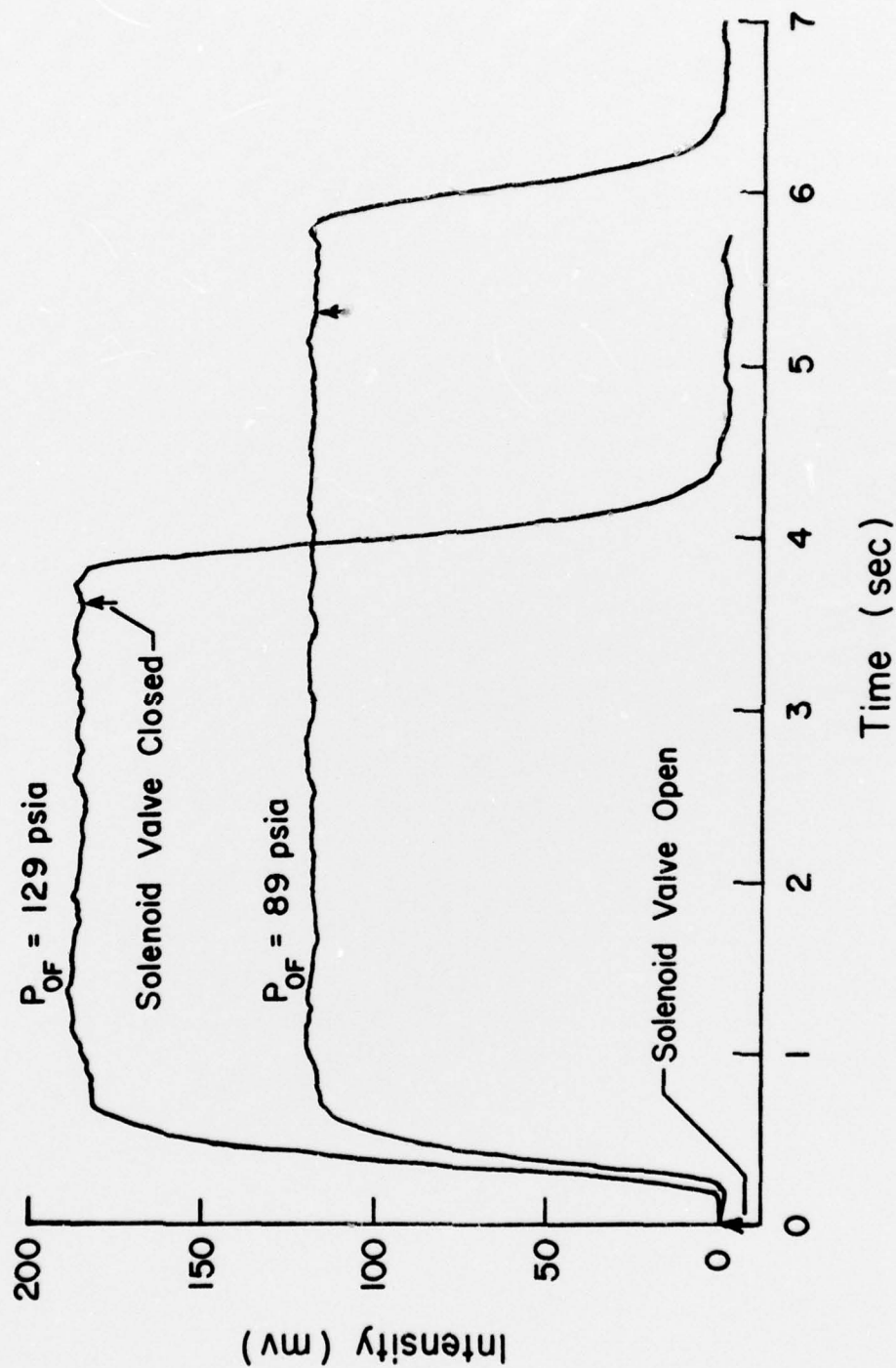


Fig. 27. Plots of Argon Ion Signal Time Response for Gas Sampled from the Reference Probe